microplastics

MDPI

Article

Enhanced Photo-Oxidative Degradation of Polyethylene Films Using Piperonyl-Functionalized TiO_2

Ricardo Acosta Ortiz *, Roberto Yañez Macías, Hortensia Maldonado Texle, Víctor Javier Cruz Delgado, Antonio Serguei Ledezma Pérez and Aída Esmeralda García Valdez

Centro de Investigación en Quimica Aplicada, Saltillo 25294, Coahuila, Mexico; roberto.yanez@ciqa.edu.mx (R.Y.M.); hortensia.maldonado@ciqa.edu.mx (H.M.T.); victor.cruz@ciqa.edu.mx (V.J.C.D.); antonio.ledezma@ciqa.edu.mx (A.S.L.P.); aida.garcia@ciqa.edu.mx (A.E.G.V.)
* Correspondence: ricardo.acosta@ciqa.edu.mx

Abstract

This study presents a surface-engineered TiO_2 photocatalyst that significantly accelerates the early stages of polyolefin oxidation. Piperonyl maleate (PipM) was synthesized and grafted onto surface hydroxyl groups of TiO_2, producing a hybrid photocatalyst (TiO_2–Pip) enriched in highly labile hydrogens. This modification enhances radical generation and enables a hydrogen-abstraction pathway that proceeds much faster than the spontaneous autoxidation typically observed in polyolefins. As a result, LDPE films containing TiO_2–Pip undergo markedly accelerated oxidation during UV aging. Hydroxyl radicals generated on the modified TiO_2 surface abstract the labile hydrogens of the piperonyl moiety, forming alkyl radicals that react with oxygen to produce peroxyl species. These peroxyl radicals promote rapid hydroperoxide formation and intensify chain-scission reactions. Gel permeation chromatography confirmed deep oxidative fragmentation, showing a reduction in Mw from 88,000 to 3300 g/mol after accelerated UV exposure. The oxidized oligomers were evaluated in fungal exposure assays, and the UV-aged films showed visible colonization by *Aspergillus niger* and *Penicillium* sp., indicating susceptibility to biodegradation. By driving LDPE oxidation to molecular weights within the range reported as microbially assimilable, the TiO_2-Pip system offers a potential strategy for reducing the environmental persistence of plastic waste; further work using microplastic-relevant particle geometries is needed to confirm its relevance to environmental microplastic mitigation.

Keywords: photodegradation; photocatalyst; modified TiO_2; LDPE; accelerated aging

Check for updates

Academic Editor: Nicolas Kalogerakis

Received: 20 August 2026
Revised: 2 October 2026
Accepted: 5 October 2026
Published: 8 October 2026

Copyright: © 2026 by the authors. Licensee MDPI, Basel, Switzerland. This article is an open access article distributed under the terms and conditions of the Creative Commons Attribution (CC BY) license.

1. Introduction

The photocatalytic activity of TiO_2 in promoting the degradation of polyolefins, especially polyethylene (PE) and polypropylene (PP), has been investigated for more than three decades [1,2]. Upon UV irradiation, TiO_2 generates electron–hole pairs that oxidize surface-adsorbed water or hydroxide ions to yield •OH radicals, while conduction-band electrons reduce molecular oxygen to $O_2\bullet^-$ and related reactive oxygen species [3,4]. These hydroxyl radicals abstract hydrogen atoms from the C–H bonds of the polyolefin backbone, producing macroradicals that subsequently undergo oxygen addition, hydroperoxide formation, and β-scission reactions. The resulting oxidative pathways lead to carbonyl accumulation, progressive chain cleavage, and mechanical embrittlement [5,6]. Early studies on LDPE and HDPE films confirmed that even low TiO_2 loadings markedly accelerate this photo-oxidative process relative to unfilled controls [7–9]. Ohtani and co-workers [10]

showed that TiO_2 embedded in PE films catalyzes hydroperoxide and carbonyl formation, with clear correlations between TiO_2 content, radical generation, and chain-scission rates. Comparable behavior has been reported for PP [11], where TiO_2-filled matrices exhibit accelerated photo-oxidative degradation and more severe surface cracking than neat PP. These findings establish TiO_2 as a highly effective pro-oxidant catalyst for polyolefins in UV-rich environments.

More recently, attention has shifted to the photocatalytic degradation of polyolefin microplastics using TiO_2-based materials, including nano-TiO_2 and TiO_2 hybrids [12–14]. Several studies have shown that TiO_2 can oxidize LDPE and HDPE microplastics in aqueous suspensions, leading to surface erosion, increased oxygen content, and the formation of lower-molecular-weight oxidation products [15,16]. A recent review by Yeszhan et al. [17] summarizes advances in the TiO_2-photocatalyzed degradation of PE microplastics, highlighting that TiO_2 promotes photooxidation, carbonyl formation, and partial mineralization of LDPE and HDPE under controlled irradiation and emphasizing the role of catalyst morphology, crystal phase, and dispersion in determining degradation efficiency. Broader reviews similarly conclude that TiO_2 is among the most effective materials for initiating the oxidative breakdown of PE and PP particles, particularly under UV or simulated solar light, and that coupling TiO_2 with other semiconductors or dopants can extend its activity into the visible region [18,19].

In previous work, our research group developed two pro-degradant additives for LDPE by functionalizing the surface of TiO_2 with organic side chains bearing highly labile hydrogens [20]. Arachidonic acid ((5Z,8Z,11Z,14Z)-icosa-5,8,11,14-tetraenoic acid) and cervonic acid ((4Z,7Z,10Z,13Z,16Z,19Z)-docosa-4,7,10,13,16,19-hexaenoic acid) were selected because both polyunsaturated fatty acids possess non-conjugated allylic hydrogens, a class of C–H bonds well known to be highly susceptible to radical hydrogen abstraction, which we hypothesized would be readily abstracted by hydroxyl radicals generated on the TiO_2 surface under UV irradiation. LDPE films containing these functionalized additives underwent rapid photo-oxidative degradation: molecular weight (Mw) decreased from 95,000 g/mol to 7730 and 4880 g/mol for arachidonic-modified TiO_2 at 1% and 3% loadings, respectively, and to 6260 and 4950 g/mol for cervonic-modified TiO_2 at the same concentrations, after 200 h of UV ageing. These results demonstrate the efficiency of polyunsaturated side chains in promoting radical-driven chain scission.

Building on this evidence, we hypothesized that incorporating even more labile hydrogens, such as benzylic or acetalic hydrogens, onto the TiO_2 surface could further accelerate degradation and reduce the molecular weight of LDPE oligomers to the 3000–4000 g/mol range. This target range is motivated by previous experimental observations linking lower-molecular-weight polyethylene oxidation products to increased microbial activity. Classic studies by Albertsson and Karlsson [21–23] reported that oxidized polyethylene became more accessible to microbial colonization as its molecular weight decreased below approximately 5000 g/mol, with oligomers in the 1000–3000 g/mol range showing measurable mineralization in soil. Subsequent studies on oxo-degradable PE reported consistent observations: Ojeda et al. [24] reported microbial growth on oxidized LDPE fragments with Mn $\approx$ 3000–4000 g/mol, while Chiellini et al. [25] observed increased biodegradation once oxidation had reduced the molecular weight below 4000 g/mol. Reviews by Lucas et al. [26] and Roy et al. [27] similarly note that the introduction of oxygenated functional groups and a reduction in molecular weight toward the $\leq$3000–5000 g/mol range are commonly associated with enzymatic attack and microbial metabolism; however, microbial colonization of a substrate does not by itself establish that the polymer carbon is being assimilated or mineralized. More recent studies report similar associations: Gewert et al. [28] describe environmental oxidation pathways that reduce polyolefins to fragments

below 5000 g/mol, a range at which microbial metabolism becomes more likely, while Shah et al. [29], Restrepo-Flórez et al. [30], Ghatge et al. [31], and Narancic and O'Connor [32] report that oxidized oligomers within the 3000–5000 g/mol window are the ones most consistently associated with microbial attack, without implying that oligomers outside this window are categorically immune to it. Taken together, these observations motivated our choice of the 3000–4000 g/mol range as an experimentally grounded target for the present study.

Despite this growing body of work, no organically modified TiO_2 system reported to date has achieved a comparable combination of rapid, deep abiotic oxidation together with direct biological validation within a single, rationally designed platform. PEG- [33] and PMMA-grafted [34] TiO_2 additives for LDPE have each reported some combination of abiotic degradation and fungal colonization, but only after considerably longer UV exposure and to a lesser extent than achieved here, while a dicarboxylic-acid-modified TiO_2 system relied on Carbonyl Index alone, without molecular-weight or biological confirmation [35]. Moreover, all these strategies, including our own prior work with polyunsaturated fatty acid modifiers [20], have relied on aliphatic allylic hydrogens as the reactive handle, leaving the far more labile benzylic and acetalic C–H bonds unexploited in TiO_2-based pro-degradant design. The novelty of the present work lies in the design of a TiO_2 surface modifier, PipM, that combines these two distinct types of highly labile hydrogens (benzylic and acetalic) with an electron-deficient maleate linker that simultaneously links the moiety to the TiO_2 surface and can act as a radical acceptor, a dual role not previously exploited in TiO_2-based pro-degradant systems. This study further evaluates whether this combined chemistry can drive LDPE oxidative fragmentation toward the molecular-weight range identified in the literature as favorable for microbial attack and assesses the resulting oxidized oligomers for evidence of fungal colonization, as a preliminary indicator of their susceptibility to biodegradation.

Although the present work is not directly focused on microplastic substrates, it builds on the demonstrated effectiveness of unmodified TiO_2 in degrading polyolefin microplastics [12–17]. On this basis, we hypothesized that a more reactive hybrid photocatalyst incorporating highly labile organic hydrogens would offer a further efficiency gain over unmodified TiO_2, motivating its evaluation, as a first step, on a well-controlled LDPE film system before extending it to microplastic substrates directly. To this end, a prodegradant additive was synthesized by reacting piperonyl alcohol with maleic anhydride to form piperonyl maleate mono-carboxylic acid (PipM), which was subsequently grafted onto the hydroxylated surface of TiO_2. The functionalized TiO_2 was melt-compounded with LDPE, and blown films were produced. The efficiency of the additive in LDPE at 1 and 2 wt% was compared with LDPE containing pristine TiO_2 at the same concentrations, and with neat LDPE, after 240 h of accelerated UV ageing in a QUV chamber. Degradation was assessed through Carbonyl Index evolution, mass loss, tensile property retention, and molecular weight changes by GPC. A biological assay was carried out using *Aspergillus niger* and *Penicillium* sp. strains to determine whether the oxidized oligomers produced during degradation could support fungal colonization.

2. Materials and Methods

2.1. Materials

The low-density polyethylene (LDPE) used in this study corresponded to grade PX-20020X, provided by PEMEX (CDMX, México). This polymer exhibits a melt flow index of 1.8–2.3 g/10 min, a density between 0.9195 and 0.9220 g/cm^3, and an average molecular weight (Mw) close to 88,000 g/mol. Titanium (IV) oxide nano powder with a particle size of 21 nm and 99.5% purity, along with toluene, hydrogen peroxide (30%), nitric acid (70%),

sodium hydroxide, piperonyl alcohol (98%) and maleic anhydride (99%), was purchased from Merck at Toluca, Mexico.

2.2. Synthesis of the Prodegradant Additive

2.2.1. Synthesis of Piperonyl Maleate (PipM)

In a 250 mL three-neck round-bottom flask, 10 g (0.065 mol) of piperonyl alcohol and 19.335 g (0.1971 mol) of maleic anhydride were reacted in a 1:3 molar ratio, using reagent-grade toluene as the solvent. The reaction mixture was stirred continuously with a magnetic stirrer for 48 h, at room temperature. After 28 h, the mixture developed an opalescent appearance, and by 36 h, gradual precipitation was observed along with a marked increase in viscosity. Throughout this period, the conversion of piperonyl alcohol was monitored. At the 48-h mark, thin-layer chromatography confirmed complete consumption of the starting alcohol, indicating full conversion under the established conditions. Upon completion, the reaction mixture was vacuum-filtered through a Büchner funnel, using the minimum necessary amount of toluene to rinse the solid product. The filtrate was then subjected to a second, rapid filtration through a gravity funnel fitted with 150 mm Whatman filter paper to remove any fine particles that may have passed through the initial filtration. The organic phase was washed with pre-chilled deionized water and transferred to a separatory funnel, maintaining equal volumes of aqueous and organic layers. Three successive washes with deionized water were performed. During the second and third washes, crystalline material formed in the organic phase; these crystals were collected and dried. The purified organic layer was then concentrated using a rotary evaporator and further dried. The three resulting solid fractions (crystals from the washes and the residue from solvent evaporation) were placed in a vacuum oven at 50 °C to complete drying. Final purification of the solid was achieved by recrystallization in toluene. This recrystallization process was repeated three times to maximize the purity of the PipM compound. The desired compound was produced at 75% yield.

2.2.2. Preparation of Hydroxyl-Enriched TiO_2 Nanoparticles (TiO_2-OH)

To increase the density of hydroxyl groups on the surface of pristine TiO_2 nanoparticles, the particles were subjected to a two-stage oxidative treatment: an alkaline stage, using hydrogen peroxide in the presence of NaOH at 50 °C for 24 h, followed by an acidic stage, using nitric acid to lower the suspension to pH 3. Typically: an aqueous 4 M sodium hydroxide solution was first prepared by dissolving 80 g of NaOH in a total volume of 500 mL of water. The mixture was stirred magnetically until a clear and uniform solution was obtained. Because the dissolution process is exothermic, the solution was cooled to 4 °C in an ice bath before proceeding. Once the desired temperature was reached, the alkaline solution was transferred to a 2 L three-neck flask equipped with a thermometer, condenser, and mechanical stirring. Then, 40 g of TiO_2 nanoparticles were added, and the resulting suspension was heated to 50 °C using an oil bath. At this temperature, 20 mL of 30% hydrogen peroxide were added dropwise through an addition funnel. The reaction was allowed to proceed for 24 h. After this period, the mixture was slowly acidified with 290 mL of nitric acid until the pH reached 3. The suspension was then left undisturbed to allow particle sedimentation. The supernatant was carefully removed with a syringe to avoid disturbing the solid phase. The recovered solid was washed repeatedly with deionized water (1.5 L total), performing three cycles of stirring, sedimentation, and decantation, until the washings reached neutral pH and all residual sodium ions were eliminated. After resting overnight, the material exhibited significantly reduced moisture content. It was then transferred to a beaker and dried in a vacuum oven at 50 °C to complete the drying process.

2.2.3. Functionalization of TiO_2-OH with PipM

A 2000 mL three-neck flask equipped with a reflux condenser, thermometer, and ultrasonic generator was charged with 10 g of TiO_2-OH nanoparticles dispersed in 500 mL of toluene. The suspension was subjected to ultrasonic irradiation for 30 min using a sonotrode to ensure homogeneous dispersion. Then, 20 g of PipM were added to the reaction flask. The mixture was heated to 60 °C for 72 h. After the reaction, stirring was stopped to allow sedimentation, and the liquid phase was carefully removed with a syringe. Ethanol was added to remove any residual PipM, and the mixture was mechanically stirred for 1 h; this washing step was repeated twice. The modified nanoparticles were finally dried under vacuum for 48 h to remove residual solvent completely.

2.3. FTIR Spectroscopy Analysis

FTIR spectra of the intermediate PipM, the functionalized TiO_2 nanoparticles, and the LDPE films were recorded on a Thermo Scientific iS10 FTIR spectrometer (Waltham, MA, USA) equipped with an ATR accessory, over the spectral range of 4000–650 cm^{-1}, at a resolution of 4 cm^{-1}, averaging 32 scans per spectrum.

2.4. Scanning Electron Microscopy (SEM)

The morphology of the pristine TiO_2 and the synthesized additives was characterized using a JEOL field-emission scanning electron microscope (JSM-7401F, Peabody, MA, USA) equipped with an EDAX Octan Plus energy-dispersive X-ray spectroscopy (EDS) detector. Samples were mounted on adhesive carbon tape prior to examination. Morphological imaging was conducted at an accelerating voltage of 5 kV and a working distance of 3 mm using secondary electron detection. Elemental composition was assessed by EDS at an accelerating voltage of 15 kV and a working distance of 8 mm.

2.5. Thermogravimetric Analysis (TGA)

The extent of TiO_2 functionalization was evaluated through thermogravimetric analysis. A TA Instruments Q500 system (New Castle, DE, USA) was used for the measurements. Samples of approximately 3–5 mg were accurately weighed and placed in the instrument's balance chamber. The thermal program consisted of heating from 30 °C to 800 °C at a constant rate of 10 °C/min. The first stage of the run was carried out under a nitrogen atmosphere (50 mL/min) up to 600 °C. Once this temperature was reached, the purge gas was switched to oxygen, and the heating continued until the final temperature of 800 °C was reached.

2.6. Preparation of Blown Films Containing the Additives

Blown LDPE films were prepared using a Brabender blow-molding system. The functionalized TiO_2 additive was incorporated into the polymer matrix at concentrations of 0, 1, and 2 wt%, and processed under identical conditions to ensure comparability. Film fabrication was carried out using a single-screw extruder (diameter: 1.90 cm; L/D ratio: 63.5) operating at 30 rpm, coupled to a Plasticorder ATR 2120 drive unit (Brabender, South Hackensack, NJ, USA). The temperature profile along the extruder was carefully controlled, with settings of 175 °C at the feed zone, 180 °C in the compression zone, 185 °C in the melting zone, and 190 °C at the die. To promote uniform dispersion of the additive within the LDPE matrix, an in-line sonotrode was connected to the extrusion system. Film blowing was performed at a take-up speed of 1 m/ min and a blow-up ratio of 5:1, using a die with a diameter of 2.54 cm. The same processing conditions were applied to produce reference films containing pristine TiO_2 at 1 and 2 wt%, ensuring consistent comparison between formulations.

2.7. Aging of Films Containing Prodegradant Additives

LDPE films incorporating the prodegradant additives were subjected to accelerated aging in a QUV/SE weathering chamber (Q-Lab, Westlake, OH, USA) equipped with UVB-313 lamps. Aging was conducted under continuous UV irradiation, with no dark or condensation cycle, following the general operating practice of ASTM G154-23 [36] Film specimens were cut to dimensions of 100 mm in length, 10 mm in width, and 150 µm in thickness, and mounted on the chamber racks at 5 cm from the lamps. The irradiance within the chamber was maintained at 0.70 W m^{-2}, and the internal temperature was controlled at 60 °C. Samples were removed at predetermined intervals to monitor the progression of degradation.

2.8. Determination of the Carbonyl Index (CI) of Aged LDPE Films

The extent of oxidative degradation in the aged LDPE films was evaluated by Fourier-transform infrared (FTIR) spectroscopy using a Thermo Scientific Nicolet 6700 spectrometer (Waltham, MA, USA). The measurements were run over the spectral range of 4000–400 cm^{-1}, at a resolution of 4 cm^{-1}, averaging 32 scans per spectrum. Oxidation was monitored by the increase in absorbance of the carbonyl region between 1780 and 1715 cm^{-1}. The absorption band at 1440 cm^{-1} was employed as an internal reference for film thickness. The carbonyl index was calculated using the baseline method according to Equation (1):

$$CI = \frac{A_{1740}}{A_{1440}} \quad (1)$$

where A_{1740} is the absorbance at 1740 cm^{-1} (carbonyl group), and A_{1440} is the absorbance at 1440 cm^{-1} (reference band).

Carbonyl Index measurements were performed in triplicate for each formulation and aging time, and results are reported as mean ± standard deviation. Statistical differences among formulations at 240 h were assessed using one-way analysis of variance (ANOVA) followed by Tukey's post hoc test (α = 0.05), performed in OriginPro 2020 academic (OriginLab Corporation, Northampton, MA, USA).

2.9. Determination of Mass Loss During the Aging of the LDPE Films

To quantify mass loss during the aging of LDPE films, each specimen was weighed with high precision both before and after exposure to the aging conditions. At predetermined intervals, samples were removed from the aging chamber to monitor the progression of degradation. Each specimen was gently cleaned of loose debris, conditioned to room temperature, and weighed using an analytical balance with a resolution of at least 0.1 mg. A measurable decrease in mass indicates that portions of the polymer matrix have undergone sufficient oxidative and chain-scission degradation to detach from the film surface. When mass loss becomes significant, it reflects the formation and subsequent removal of highly embrittled, low-molecular-weight fragments generated during advanced stages of photo-oxidation. Tracking this mass loss over time provides a sensitive metric for assessing the extent of LDPE degradation under the selected aging conditions. Total Specimen Mass Loss was calculated according to Equation (2):

$$Total\ Specimen\ Mass\ Loss = \frac{m_0 - m_t}{m_0} \times 100 \quad (2)$$

where m_0 is the initial mass of the specimen and m_t is its mass after t hours of UV aging. Mass-loss measurements were performed in duplicate (n = 2) for each formulation at each aging time point. The reported value corresponds to the average of the two replicate

measurements, and error bars in corresponding figure represent the standard deviation calculated from the two replicate values.

2.10. Determination of Molecular Weight Using Gel Permeation Chromatography

A gel permeation chromatography (GPC) analysis of the LDPE films was carried out using an Agilent PL-GPC 220 system (Santa Clara, CA, USA). Each polymer sample (25 mg) was dissolved in 15 mL of trichlorobenzene and maintained at 140 °C for two hours to ensure complete solubilization. The solutions were subsequently passed through 0.5 µm stainless-steel filters to remove any particulates prior to analysis. Molecular weight determination was performed with a refractive-index detector, and calibration was based on a set of ten polystyrene standards covering a molecular-weight range from 1260 to 3,600,000 Da. After filtration, 200 µL aliquots of each solution were injected at 140 °C into the GPC instrument equipped with three PL-Gel 10 mm Mixed-B LS columns arranged in series.

2.11. Determination of Tensile Properties of the Films

The tensile degradation of the aged LDPE films was evaluated according to ASTM D882-18 [37] using a United Materials Testing instrument (Beijing, China) equipped with an environmental chamber. Specimens were stretched at a crosshead speed of 50 mm min^{-1} with an initial grip separation of 50 mm. All measurements were performed under controlled laboratory conditions (20 °C and 65% relative humidity). Five replicates were tested for each condition, and the reported values correspond to the average of these measurements. Statistical differences among formulations at each aging time point were assessed using one-way analysis of variance (ANOVA) followed by Tukey's post hoc test ($\alpha = 0.05$), performed in OriginPro (OriginLab Corporation, Northampton, MA, USA).

2.12. Determination of the Aerobic Biodegradability of Degraded LDPE Films

The aerobic biodegradability of the degraded oligomers was assessed following the ASTM D5247-92 standard [38] which outlines the procedure for evaluating the biological assimilation of oxidized polymer fragments under aerobic conditions. After UV accelerated aging, the degraded films were directly exposed to microorganisms in a defined liquid medium for a minimum of 14 days and up to 28 days. In the present study, this window was deliberately extended to 30 days, two days beyond the standard maximum, to allow additional time for fungal colonization to develop and to provide a more conservative assessment of the film surfaces. Fungal colonization was assessed at the end of this extended 30-day incubation period. During this period, the cultures were periodically inspected to document microbial growth both in the test medium and on the surface of the plastic material.

The biological material described above was propagated from lyophilized stocks obtained from the original ATCC strain. Each lyophilized vial was used to inoculate Petri dishes containing potato dextrose agar (PDA) as the growth medium, which were then incubated at 28 °C for one week until full colony development and sporulation were achieved. After one week of microorganism propagation, spore suspensions free of mycelium were prepared for each fungal strain. Then, 10 mL of sterile physiological saline solution (0.85% *w*/*v* NaCl in distilled water) weas added to each Petri dish, and the agar surface was gently scraped to detach the biological material. The resulting suspension was transferred into labeled Erlenmeyer flasks and brought to a final volume of 100 mL. To remove residual nutrients from the culture medium, each suspension underwent four centrifugation–washing cycles (14,000 rpm for 15 min, followed by a 10-min decanting period and washing with 100 mL of physiological saline solution per cycle). To obtain a spore suspension free of mycelial fragments, the mixture obtained from the plate scrapings

(spores + fungal mycelium) was filtered through a device consisting of a sterile funnel packed with sterile hydrophobic cotton. Each spore suspension was then resuspended in 50 mL of sterile water. Spore viability after filtration was verified by the plate colony count method, and spore counts were performed using a Neubauer hemocytometer, with the suspensions adjusted and verified to a final concentration of 5000 spores/mL immediately prior to inoculation. This standardized suspension was used as the inoculum for the biodegradation test.

The materials selected for evaluation were first sterilized by immersion in a 70% ethanol solution for 20 min. It was then decanted, rinsed with sterile distilled water, decanted again, and dried in an oven at 50 °C for 24 h. The dried material was stored in a clean container until use. For the biodegradation study, 250 mL Erlenmeyer flasks were prepared, each containing 60 mL of a mineral salt medium (MSM) supplemented with a nitrogen source but lacking any carbon source, so that the test material would serve as the sole carbon source [39]. For each microorganism evaluated, the following experimental treatments were prepared:

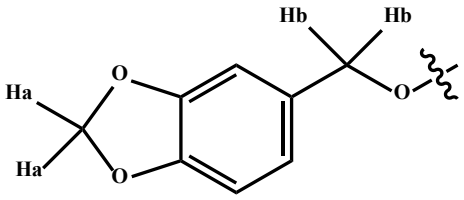
(a) Positive control (2 flasks): MSM + glucose + fungus
(b) Negative control 1 (2 flasks): MSM without glucose + fungus
(c) Negative control 2 (2 flasks): MSM + degraded LDPE + no fungus
(d) Negative control 3 (2 flasks): MSM + non-degraded LDPE + no fungus
(e) Degraded LDPE sample (3 flasks): MSM + 0.1 g degraded LDPE + fungus
(f) Non-degraded LDPE sample (3 flasks): MSM medium + 0.1 g non-degraded LDPE + fungus

Before inoculation, all flasks were incubated in a mechanical shaker at 30 °C and 150 rpm for 24 h to verify the absence of contamination. Once the culture medium was confirmed to be free of turbidity, the flasks were inoculated with standardized spore suspensions (5000 spores/mL), using *Aspergillus niger* (ATCC-6275) for one series and *Penicillium* sp. (ATCC-52180) for the other. The inoculated flasks were then incubated under the same controlled conditions for a period of 30 days.

3. Results

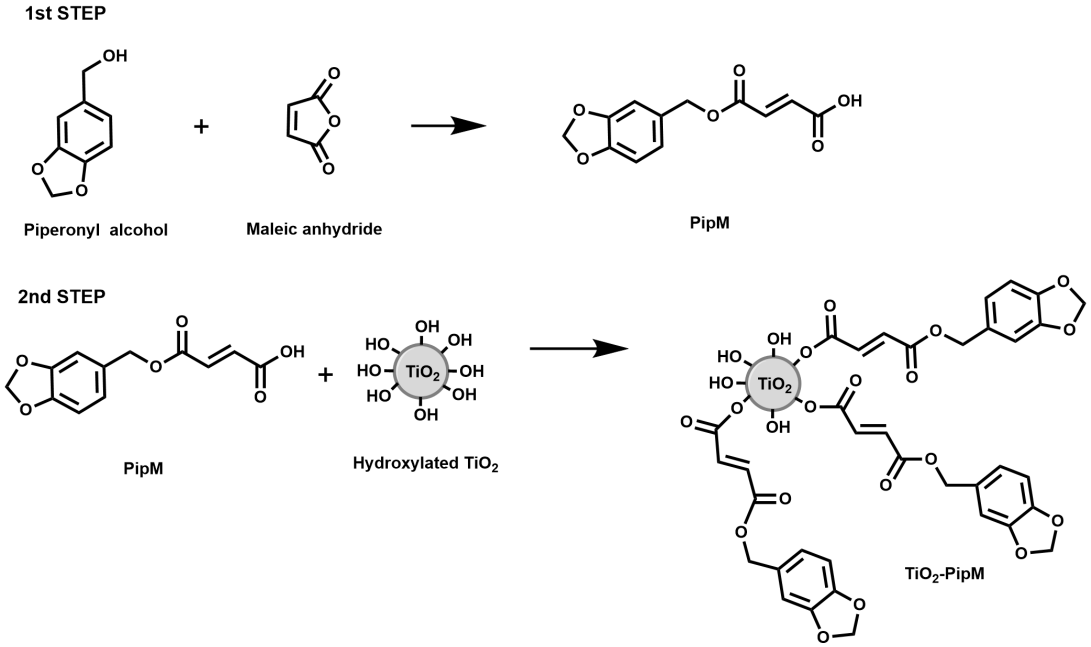
3.1. Synthesis and Characterization of the Titanium Dioxide-Based Additive TiO_2-Pip

In this study, a pro-degradant additive based on TiO_2 functionalized with a piperonyl moiety was synthesized. TiO_2 is a well-known photocatalyst that generates hydroxyl radicals, regarded as the most potent oxidizing species known, and can easily promote rapid degradation of plastic materials [40]. The design of the additive proposed in this research leveraged this intrinsic property of TiO_2. The strategy involved introducing moieties bearing labile hydrogen atoms onto the TiO_2 surface. Piperonyl alcohol was selected as the functionalizing agent. This compound contains two distinct types of labile hydrogen atoms: benzylic hydrogens, located on the methylene group bonded to both the aromatic ring and the oxygen atom, and two acetal-type hydrogens, bonded to two oxygen atoms within the second ring of the piperonyl alcohol structure, as shown in Scheme 1.



Scheme 1. Piperonyl moiety with labile hydrogens: benzylic hydrogens (Hb) and acetalic hydrogens (Ha).

To graft the piperonyl moiety onto the TiO_2 surface, a terminal carboxylic group must first be introduced (see Scheme 2). This was accomplished by reacting the piperonyl alcohol with an excess of maleic anhydride, which undergoes nucleophilic ring opening to yield a maleic monoester bearing a free carboxylic acid group (Step 1). The resulting carboxylic acid functionality reacts with the hydroxyl groups in the surface of TiO_2 through condensation reactions (Step 2). These reactions generate a robust organic–inorganic interface in which the piperonyl fragment is anchored to the TiO_2 nanoparticle via a maleate linker.



Scheme 2. Synthetic Methodology to prepare the prodegradant additive TiO_2-Pip.

To promote selective mono-esterification of maleic anhydride and suppress formation of the corresponding diester, the reaction was carried out using an excess of anhydride. Upon completion of the reaction, a solid precipitate was observed; this material was isolated and characterized, confirming that it corresponded to the desired product, PipM. The excess maleic anhydride underwent hydrolysis during the aqueous washing step and remained dissolved in the water phase. PipM was purified through three successive recrystallizations, affording the pure compound in 75% yield. Structural confirmation was obtained by proton nuclear magnetic resonance spectroscopy (^{1}H NMR), and the corresponding spectrum is shown in Figure 1. The aromatic protons H_5, H_6, and H_7 appear at 6.83, 6.89, and 6.90 ppm, respectively. The vinyl protons of the maleate fragment, H_3 and H_4, are observed as two coupled doublets at 6.48 and 6.39 ppm. The presence of two distinct resonances is consistent with the mono-esterified structure; in contrast, formation of the symmetric diester would render the vinyl protons chemically equivalent, producing a single singlet. In the monoester, one vinyl proton is adjacent to an ester group while the other is adjacent to a carboxylic acid, accounting for their different chemical environments. The acetalic protons of the heterocyclic ring appear as a singlet at 6.01 ppm, indicating their equivalence. Similarly, the benzylic protons resonate as a singlet at 5.22 ppm. The signal above 7 ppm corresponds to the deuterated solvent ($CDCl_3$). The absence of additional peaks confirms the high purity of PipM.

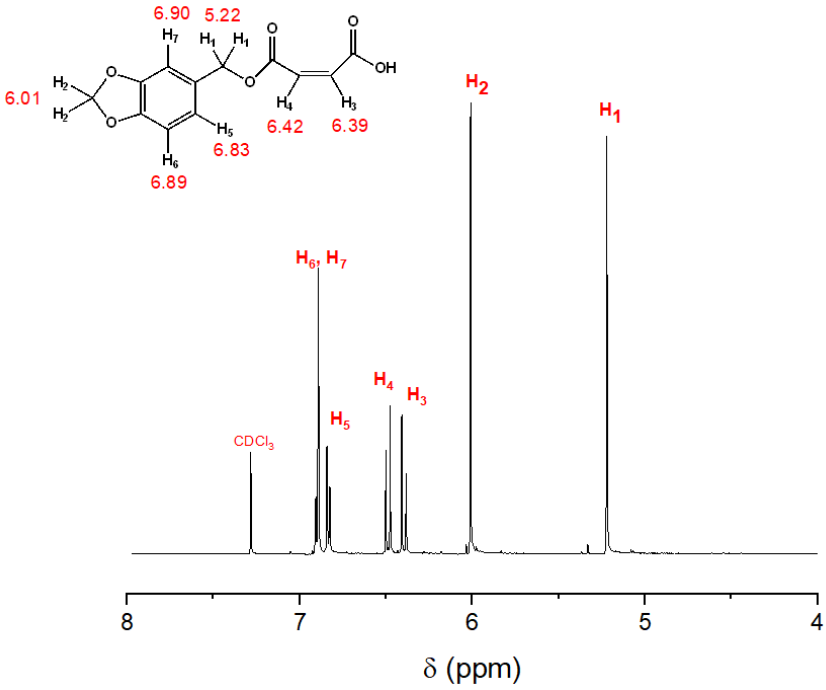


Figure 1. ^{1}H NMR spectrum of PipM run in $CDCl_3$. Red labels correlate the protons in the chemical structure with their corresponding signals.

PipM was further characterized by FTIR spectroscopy using the ATR technique (Figure 2). The resulting spectrum exhibits the diagnostic vibrational features expected for the monoester. A strong absorption band at 1727 cm^{-1} corresponds to the ester carbonyl stretching vibration. Although a distinct carbonyl band from the residual carboxylic acid group would normally be anticipated, it is likely to overlap with the ester carbonyl due to their close spectral proximity. Two characteristic absorptions associated with the C=C double bond appear at 3051 cm^{-1} and 1634 cm^{-1}, confirming the retention of the alkene functionality. Additionally, the C–O stretching bands at 1245 cm^{-1} and 1167 cm^{-1} further support the successful formation of the monoester structure. Together, these features provide strong spectroscopic evidence for the correct synthesis of PipM.

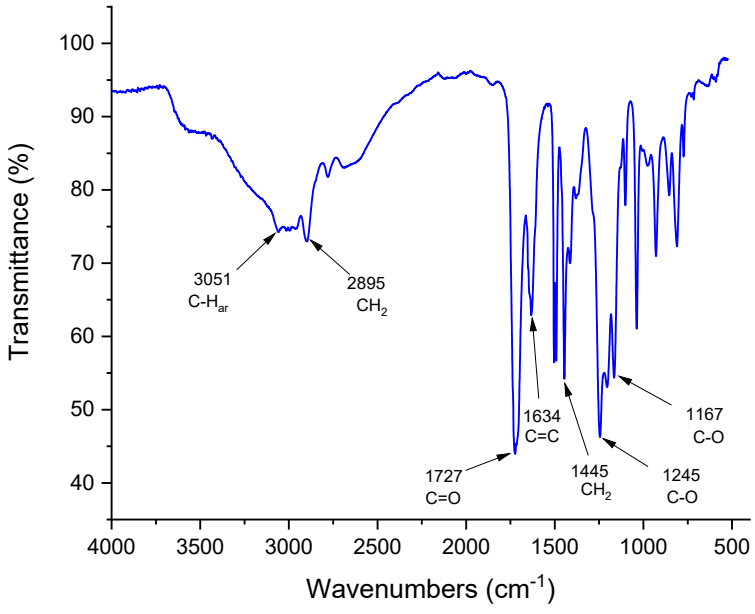


Figure 2. FTIR spectrum of PipM run with an ATR accessory.

3.2. Preparation of the Piperonyl Modified TiO_2 (TiO_2-Pip)

Once the intermediate PipM was obtained, it was used to functionalize the hydroxyl-rich TiO_2–OH by reacting their hydroxyl groups with an excess of PipM in toluene as the solvent. After 72 h, the resulting TiO_2–Pip material was thoroughly washed with ethanol to remove any unreacted PipM. FTIR analysis confirmed the successful surface modification of TiO_2. Figure 3 depicts a comparison between the FTIR spectra of pure TiO_2 and TiO_2-Pip. Pure TiO_2 shows only the characteristic bands at 3458 cm^{-1} and 1636 cm^{-1}, corresponding to surface hydroxyl groups, along with a broad band at 734 cm^{-1} attributed to the Ti–O–Ti lattice vibrations. In contrast, the spectrum of TiO_2–Pip retains these features but also displays additional bands associated with the piperonyl moiety. These include the absorption at 2932 cm^{-1}, assigned to aliphatic C–H stretching of benzylic protons, and a band at 1724 cm^{-1}, which can be attributed to the carbonyl moiety of the ester groups formed through the reaction between TiO_2 surface hydroxyls and the carboxylic acid group of PipM. The band at 1638 cm^{-1} corresponds to the maleic double bond, while the absorption at 1411 cm^{-1} is consistent with methylene group vibrations. These spectral features provide clear evidence of the successful functionalization of TiO_2 with PipM.

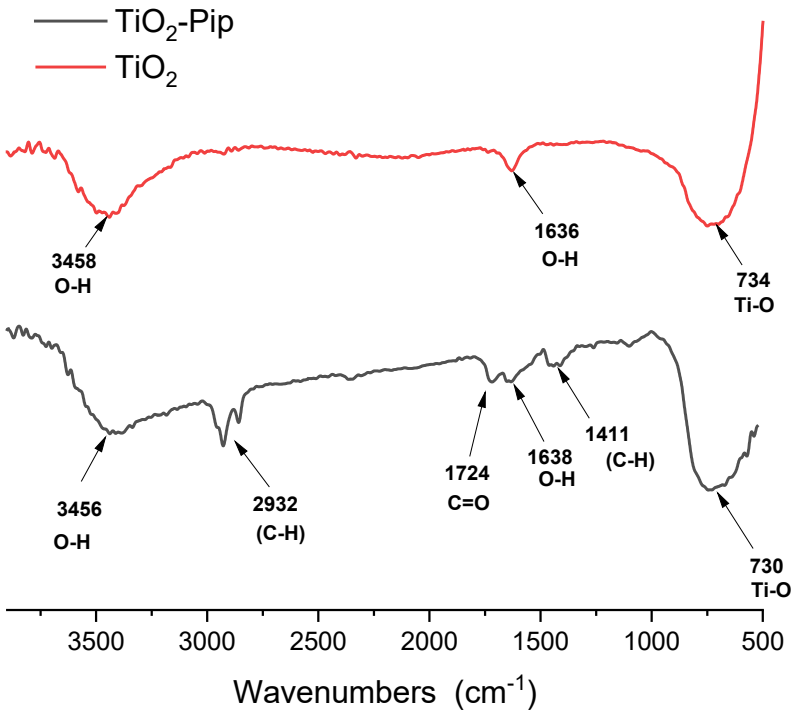


Figure 3. FTIR spectrum of TiO_2-Pip obtained using the ATR accessory.

The XPS and EDS analyses of TiO_2-Pip confirms the successful functionalization with the piperonyl moiety, as shown in Figure 4. Pristine TiO_2 exhibits only the characteristic Ti2p, O1s, and Ti2s signals, in the photoelectron spectrum. In contrast, TiO_2-Pip displays an additional C1s peak arising from the organic carbon introduced by the piperonyl group, together with the Ti and O signals, thereby corroborating the surface modification of the oxide. A similar result was obtained from the EDS analysis of TiO_2-Pip, where an additional carbon peak, corresponding to 13.42 wt%, could clearly be observed alongside the Ti and O peaks, further supporting the successful functionalization.

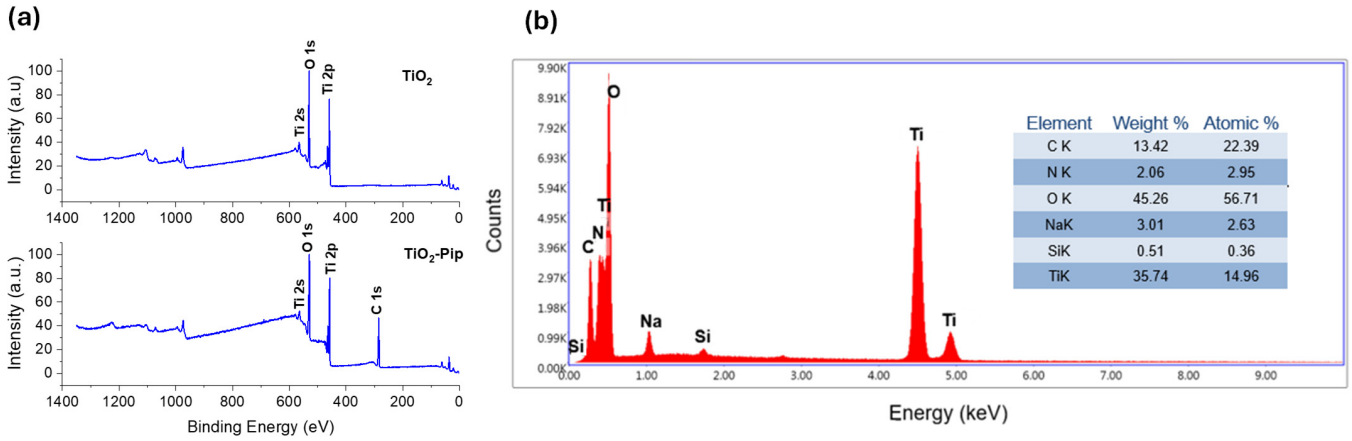


Figure 4. (**a**) Comparison of XPS Survey scans of pure TiO_2 and surface modified TiO_2-Pip; (**b**) EDS of TiO_2-Pip.

3.2.1. TGA Analysis of TiO_2-Pip

The degree of TiO_2 functionalization with PipM was evaluated by TGA. As the temperature increases, the organic moieties grafted onto the oxide surface undergo thermal decomposition, leaving only the inorganic TiO_2 residue. The corresponding thermogram is shown in Figure 5. At low temperatures, a slight mass loss is observed, which can be attributed to the release of physically adsorbed moisture. Upon further heating, a gradual decrease in mass occurs, corresponding to the thermal degradation of the piperonyl groups attached to the TiO_2 surface. This decomposition accounts for approximately 12% mass loss. Beyond 500 °C, no additional significant mass changes are detected, indicating complete removal of the organic fraction. Notably, this 12% value is consistent with the elemental composition obtained by EDS, confirming the successful functionalization of TiO_2 with PipM.

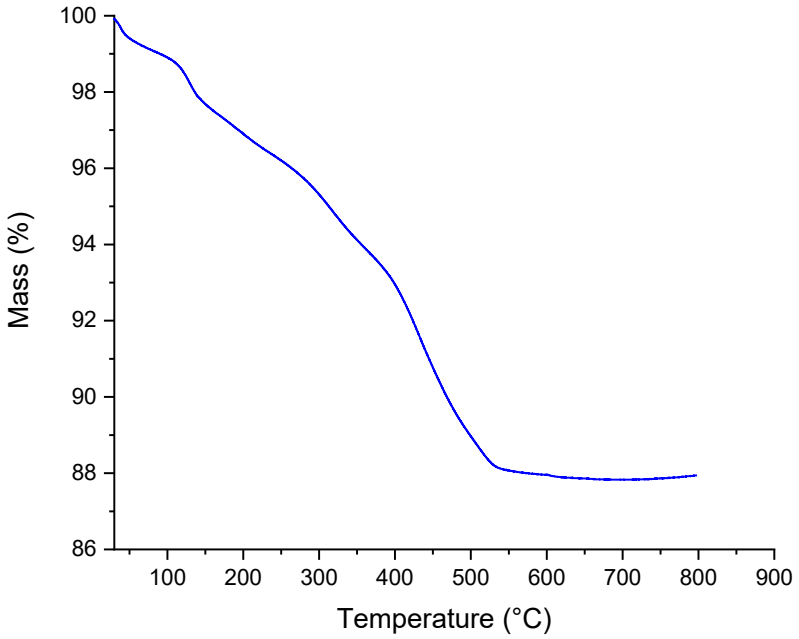


Figure 5. Thermogram of the decomposition of TiO_2-Pip.

This organic-to-inorganic composition has direct implications for the formulation of the LDPE films discussed in subsequent sections. Since the functionalized additive contains ~88% TiO_2 and ~12% PipM by mass, the effective inorganic TiO_2 content incorporated into

the LDPE films is lower than the nominal loading of TiO_2-Pip: the 1 wt% and 2 wt% nominal loadings correspond to effective TiO_2 contents of approximately 0.88 wt% and 1.76 wt%, respectively, both lower than the corresponding pristine-TiO_2 formulations prepared at the same nominal 1 and 2 wt% loadings.

3.2.2. Morphology of TiO_2-Pip

The morphology of the prepared TiO_2-Pip was determined using the SEM technique. Figure 6 depicts a comparison of the micrographs corresponding to pure TiO_2 and TiO_2-Pip at different magnifications. Micrographs (a) and (b) show aggregates of TiO_2, small, roughly spherical or polyhedral particles, of 10–50 nm in size. Due to high surface energy and abundant surface hydroxyl groups, pure TiO_2 nanoparticles cluster into dense aggregates. The unmodified TiO_2 shows clean particle boundaries and no surface films, consistent with the absence of organic modifiers. In the case of TiO_2-Pip the organic functionalization leads to larger aggregates because the coating alters surface charge and reduces electrostatic repulsion. Functionalized TiO_2-Pip appears with slightly smoother or "blurred" particle edges, consistent with an organic coating. The piperonyl monoester forms an organic shell around TiO_2, which is clearly shown in micrographs (c) and (d).

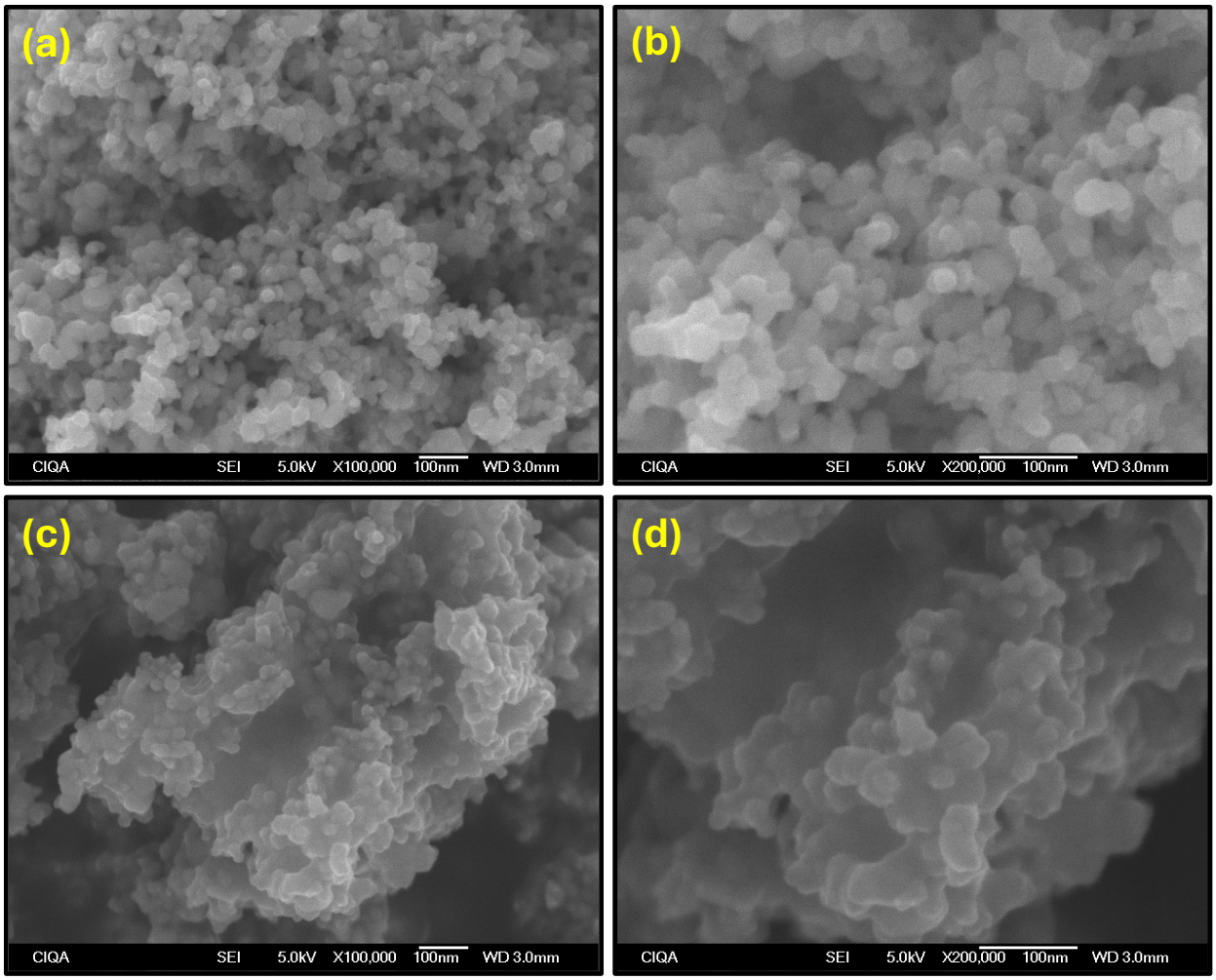
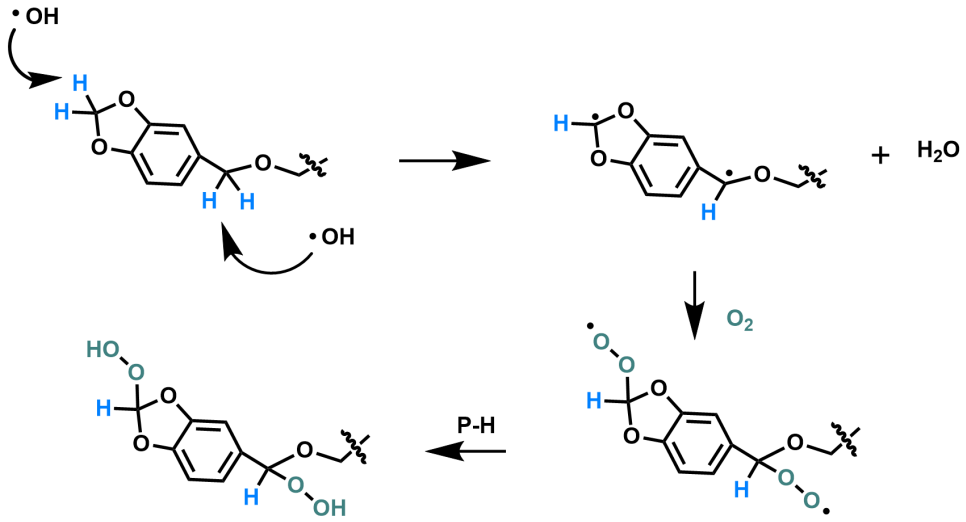


Figure 6. SEM micrographs of pure TiO_2 at ×100,000 (**a**) and at ×200,000 (**b**), and TiO_2-Pip at ×100,000 (**c**) and at ×200,000 (**d**).

3.3. Photo-Oxidation of the LDPE Films

The proposed mode of action of this pro-degradant agent is depicted in Scheme 3. Under UV irradiation, hydroxyl radicals generated on the surface of the modified TiO_2 readily abstract the highly labile benzylic and acetalic hydrogens [41,42] of the pendant piperonyl groups, producing resonance-stabilized alkyl radicals. These radicals react almost instantaneously with molecular oxygen to yield peroxyl radicals, which are subsequently converted into hydroperoxides. Because this photocatalytically driven hydrogen-abstraction pathway is significantly faster than the spontaneous formation of alkyl radicals within the polymer matrix, the reactive intermediates derived from TiO_2–Pip effectively bypass the slow initiation step characteristic of conventional autoxidation. As a result, the polymer enters the autoxidation cycle rapidly, leading to a markedly accelerated degradation process.



Scheme 3. Proposed Mechanism of Action of the prodegradant additive TiO_2-Pip.

The maleic double bond that anchors the piperonyl moiety to the TiO_2 surface contributes actively to the autoxidation of LDPE. Owing to its electron-deficient nature, the maleate double bond is expected to behave as an efficient radical acceptor [43], capturing alkyl and peroxyl radicals generated during UV exposure and photocatalysis. This interaction would promote the formation of stabilized maleate-centered radicals that facilitate further propagation of the oxidative cycle. In addition, the strong electron-withdrawing character of the maleate group increases the lability of the benzylic and acetalic hydrogens of the piperonyl unit, enhancing hydrogen abstraction by •OH and ROO• species. As a result, the maleic linkage not only attaches the organic moiety to the TiO_2 surface but also amplifies radical generation and propagation, accelerating hydroperoxide formation, decomposition, and ultimately chain scission in LDPE. This mechanistic picture is based on established structure–reactivity precedents and observed degradation kinetics, rather than on direct spectroscopic confirmation. Confirming a radical mechanism of this kind typically requires additional experimental evidence, such as radical-scavenging experiments (e.g., with isopropanol or benzoquinone to selectively suppress •OH or $O_2•^-$) and fluorometric or EPR-based direct detection of the radical species involved, as demonstrated in studies of other radical-mediated advanced oxidation systems [44]. Such experiments were not performed in the present study and are proposed as a direction for future work to directly validate the mechanism described here.

3.3.1. Determination of the Degree of Oxidation of the LDPE Films Under Accelerated UV Aging Using the Carbonyl Index Method

The prepared oxo-degradable LDPE films were subjected to UV aging in a QUV chamber using only the radiation cycle. During accelerated UV aging, low-density polyethylene (LDPE) films undergo progressive photo-oxidative degradation, evidenced by the formation of oxygen-containing functional groups such as hydroxyl groups, carboxylic acids, and carbonyl-type compounds such as esters, lactones, ketones, and aldehydes, into the polymer backbone. The accumulation of the carbonyl species produces a characteristic increase in the infrared absorption band within the 1780–1700 cm^{-1} region. Quantifying the growth of this band (expressed as the carbonyl index CI), provides a reliable measure of the extent of oxidative degradation. Higher CI values correlate strongly with embrittlement, loss of tensile strength, and reduced elongation at break, reflecting the progressive breakdown of the polymer chains. Figure 7 shows the evolution of the carbonyl index (CI) for the UV-aged LDPE films. Overall, the films containing TiO_2-Pip exhibited a substantially faster and more pronounced increase in CI throughout the entire UV-exposure period. During the first 100 h of aging, the CI of the TiO_2-Pip films increased slightly but consistently more rapidly than that of both the pristine TiO_2 formulations and the control film. This early rise provides clear evidence of the accelerating effect imparted by the labile hydrogens present in the piperonyl side-chain, which facilitate rapid hydrogen abstraction of the polymer, by the hydroxyl radicals generated on the TiO_2 surface under UV irradiation. In contrast, the control film and the samples containing unmodified TiO_2 at 1% and 2% showed only minimal increases in carbonyl absorption during this initial period, indicating a slower onset of oxidation. After approximately 100 h, however, all films entered a phase of accelerated oxidative degradation. Notably, the TiO_2-Pip formulations reached very high CI values of 5.6 ± 0.56 and 5.36 ± 0.45 (for 2% and 1%, respectively) after 240 h of UV exposure, confirming their strong pro-oxidant behavior. Films containing pristine TiO_2 displayed intermediate CI values (3.9 ± 0.67 and 3.49 ± 0.73 for 2% and 1%, respectively), while the additive-free film exhibited the lowest degree of oxidation, with a CI of 1.49 ± 0.34 at the same exposure time. At 240 h, these differences among formulations were statistically significant (one-way ANOVA, F = 25.54, $p = 3.13 \times 10^{-5}$).

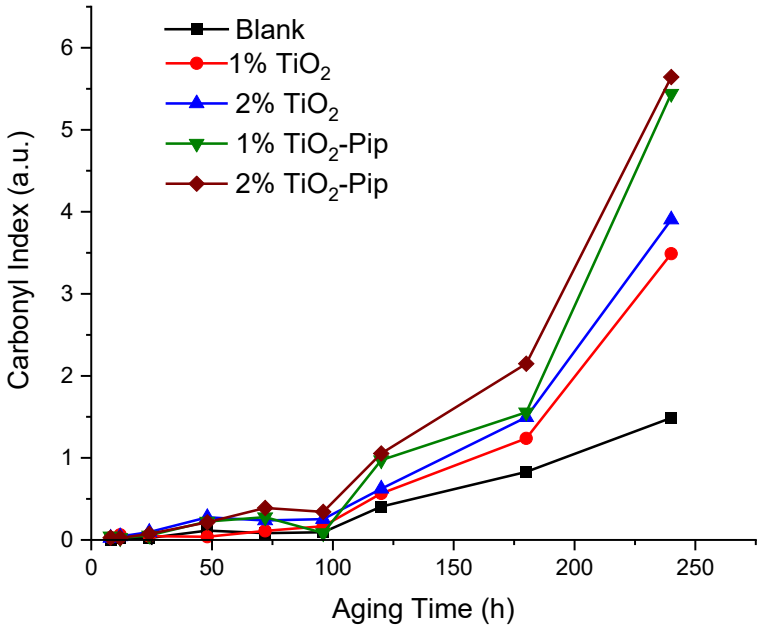


Figure 7. Carbonyl Index vs. Aging Time of the films formulated with the pristine TiO_2 and additive TiO_2-Pip compared with the films without additives.

These results demonstrate that TiO_2-Pip is significantly more effective than pristine TiO_2 in promoting photo-oxidation, consistent with the combined contribution of photocatalytic hydroxyl-radical generation and abstraction of the highly reactive benzylic and acetalic hydrogens on the modifier. The CI data also reveal a distinct induction period of approximately 100 h for the TiO_2-Pip films, after which the rate of carbonyl accumulation increases sharply, consistent with the accumulation and subsequent decomposition of hydroperoxides. These findings confirm that surface functionalization of TiO_2 with piperonyl groups greatly enhances its pro-degradant efficiency, leading to faster initiation and propagation of the autoxidation process in LDPE.

3.3.2. Determination of Mass Loss During the UV Aging of the PE Films

The analysis of mass loss during UV aging is a straightforward yet highly informative method for evaluating the extent of polymer degradation and comparing the pro-oxidant efficiency of additives. In this procedure, polymer films are carefully weighed before exposure and then periodically weighed after defined intervals of UV irradiation. Any reduction in mass reflects the loss of low-molecular-weight fragments, volatile oxidation products, or surface material that has undergone extensive chain scission. Figure 8 depicts the graph of the mass loss vs. UV aging time of five PE samples.

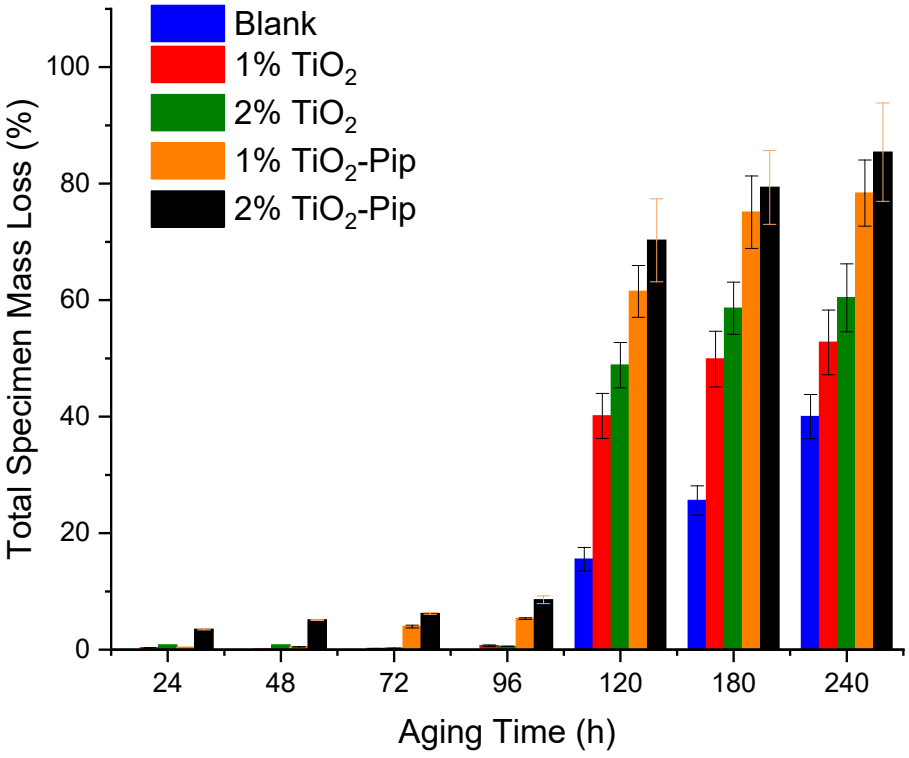


Figure 8. Total Specimen Mass Loss vs. Aging Time of LDPE films with and without prodegradant additives: blank, pristine TiO_2 at 1% and 2% *w*/*w*, TiO_2-Pip at 1% and 2% *w*/*w*.

The mass-loss analysis of the UV-aged films is consistent with the CI results. During the first 100 h of exposure, the films containing TiO_2-Pip exhibited a modest but noticeable increase in mass loss (≈5–8%), whereas the control film and those formulated with pristine TiO_2 showed only negligible changes. This early divergence suggests that the presence of labile hydrogens in the piperonyl side-chain significantly accelerates the autoxidation of PE compared with unmodified TiO_2. After this initial period, all formulations entered a regime of rapid degradation, reflected by a sharp rise in mass loss. Nevertheless, the same trend persisted throughout the entire aging process: films containing TiO_2-Pip

consistently displayed the highest mass loss at every exposure time. After 240 h of UV irradiation, the mass loss reached 78 ± 5.6% and 85 ± 8.4% for the films with 1% and 2% TiO_2-Pip, respectively. In contrast, the films with pristine TiO_2 showed substantially lower mass losses of 52 ± 5.5% (1%) and 60 ± 5.8% (2%). The additive-free film exhibited the lowest degradation, with a final mass loss of 40 ± 3.8% at 240 h. These results demonstrate the superior pro-degradant efficiency of TiO_2-Pip, which promotes faster chain scission and volatilization of degradation products compared with pristine TiO_2 and the blank formulation.

Given that TiO_2 is non-volatile, the mass loss observed cannot be attributed to volatilization of the inorganic component itself. It is most likely the result of two contributions arising from photo-oxidative chain scission: the release of volatile low-molecular-weight oxidation products, and the physical detachment of embrittled polymer fragments from the film surface [45,46]. Morphological evidence supporting this interpretation is presented in Section 3.5. Because TiO_2-Pip is embedded within the polymer matrix rather than confined to the surface, these detaching fragments are expected to carry entrapped TiO_2-Pip particles along with them, together with volatile low-molecular-weight oxidation products generated during chain scission.

3.3.3. GPC Analysis of Degraded PE Films

The molecular-weight data listed in Table 1 reveals distinct degradation behaviors among the LDPE films as a function of formulation and UV exposure time. In all cases, UV irradiation induces a progressive decrease in both weight-average molecular weight (Mw) and number-average molecular weight (Mn), consistent with photo-oxidative chain scission as the dominant degradation pathway. However, the rate and extent of molecular-weight loss differ markedly between the control film, the films containing pristine TiO_2, and those incorporating TiO_2-Pip. The blank film exhibits an overall decrease in Mw and Mn over the 240 h exposure period, although this trend is not strictly continuous: Mw shows a transient increase at 60 h (from 88,782 to 99,612 g/mol) before decreasing at longer exposure times, consistent with the simultaneous occurrence of chain scission and radical-recombination crosslinking reactions typically reported during the early stages of polyolefin photo-oxidation, particularly in unmodified films lacking a pro-oxidant catalyst to accelerate hydroperoxide decomposition and drive scission-dominated degradation from the outset [47,48]. By 240 h, Mw decreases to 30,118 g/mol and Mn drops from 23,391 to 2970 g/mol, accompanied by a sharp rise in polydispersity (IPD = 10.1). This overall pattern is characteristic of random chain scission, where the formation of carbonyl groups and hydroperoxides progressively weakens the polymer backbone once scission becomes the dominant pathway. The high IPD at 240 h indicates the coexistence of both heavily degraded low-molecular-weight fragments and residual high-molecular-weight chains. In the case of the films compounded with pristine TiO_2, it was observed to have a significant reduction in molecular weight relative to the blank. After only 60 h, Mw drops to 27,288 g/mol (1%) and 24,970 g/mol (2%), which are values far below those of the control at the same exposure time. This confirms the well-known photocatalytic activity of TiO_2, which generates hydroxyl radicals capable of abstracting hydrogen atoms from the polymer chains, thereby initiating the autoxidation cycle more efficiently. By 240 h, the Mw values fall to 9235 g/mol (1%) and 7395 g/mol (2%), indicating extensive chain scission. Interestingly, the IPD values at 240 h (3.85 and 3.32) are lower than that of the blank, suggesting a more uniform degradation pattern, likely due to the catalytic nature of TiO_2 promoting widespread radical formation throughout the matrix.

Table 1. Analysis of the diminution of molecular weight of the different UV aged films.

Sample	Time 0			Time 60 h			Time 120 h			Time 240		
	Mw	Mn	IPD	Mw	Mn	IPD	Mw	Mn	IPD	Mw	Mn	IPD
Blank	88,782	23,391	3.80	99,612	18,066	5.51	56,357	12,157	4.63	30,118	2970	10.1
PE + TiO_2 1%	87,312	21,247	4.11	27,288	5110	5.34	14,476	2755	5.25	9237	1938	3.85
PE + TiO_2 2%	82,025	20,000	4.10	24,970	4853	5.15	11,172	2467	4.52	7395	1251	3.32
PE + TiO_2-Pip 1%	88,314	18,663	4.73	16,331	3892	4.20	10,299	2473	4.16	4796	1122	4.27
PE + TiO_2-Pip 2%	84,961	18,399	4.62	16,218	4467	3.63	8549	2052	4.16	3353	949	3.53

Note: The Mw, Mn and IPD values reported here are polystyrene-equivalent and were not confirmed by an orthogonal, absolute method such as high-temperature SEC-MALLS or NMR end-group analysis; the reported reductions in molecular weight should therefore be interpreted as relative trends across formulations and aging times, rather than as absolute molar mass values. Confirmation of the key Mw values (particularly the 3300–3400 g/mol range) by an orthogonal method is proposed as a target for future work.

The films containing TiO_2-Pip show the most dramatic decrease in molecular weight, confirming the strong pro-degradant effect of the surface modification. After 60 h, Mw values fall to 16,331 g/mol (1%) and 16,218 g/mol (2%), already approaching the levels observed in pristine TiO_2 films at much longer exposure times (120 h). By 240 h, Mw reaches 4796 g/mol (1%) and 3353 g/mol (2%), representing the lowest molecular weight among all formulations. The Mn values also collapse to 1122 and 949 g/mol, respectively, indicating extensive fragmentation into very short chains and oligomers. This enhanced degradation is attributed to the piperonyl moiety, which introduces highly labile benzylic and acetalic hydrogens. These hydrogens are readily abstracted by hydroxyl radicals generated on the TiO_2 surface under UV irradiation. As a result, TiO_2-Pip acts as a radical-transfer catalyst, accelerating the formation of alkyl radicals on the polymer backbone and promoting rapid autoxidation. It is worth noting that this substantial reduction in molecular weight occurs within the first 60 h of UV exposure, i.e., within the time window that CI and Mass-Loss measurements (Sections 3.3.1 and 3.3.2) identify as an induction period of approximately 100 h. This apparent discrepancy arises from the different nature of these techniques: CI and Mass-Loss track the accumulation of oxidation products and the physical loss of material, respectively, both of which become clearly measurable only once degradation has progressed sufficiently, whereas GPC directly probes the molecular weight of the polymer backbone and is therefore more sensitive to chain scission at earlier stages. This decoupling between early chain scission and delayed carbonyl accumulation is well documented in polyolefin photo-oxidation: extensive molecular-weight reduction has been reported to occur before appreciable CI can be detected in polyethylene, without any associated increase in carbonyl concentration [49]. Accordingly, the present GPC data indicate that chain scission begins well before it is reflected in the CI or Mass-Loss trends, rather than contradicting the induction period identified by those two techniques; the induction period should thus be understood as applying specifically to the onset of detectable carbonyl accumulation and mass loss, not to the onset of chain scission itself. This distinction is important, as it confirms that TiO_2-Pip is the most effective pro-degradant system evaluated, initiating backbone cleavage earlier than either of the other two formulations.

3.4. Determination of Loss of Tensile Properties of UV Aged Films

Elongation at maximum load proved to be an effective method for evaluating the extent of UV-induced degradation in the LDPE films. Prior to UV exposure (0 h), elongation was statistically equivalent across all five formulations (one-way ANOVA, p = 0.644),

confirming that the incorporation of pristine or functionalized TiO_2 does not by itself alter the initial ductility of the LDPE films.

The results clearly show that the polyethylene films containing TiO_2 and TiO_2-Pip underwent a much more rapid decline in tensile performance than the additive-free control. At 24 h, all TiO_2-containing formulations (pristine and functionalized) showed a significant reduction in elongation relative to the blank (one-way ANOVA, Tukey's HSD, $p < 0.05$), but did not differ significantly from one another, both dropping sharply to values near 0.08–0.10 mm/mm, corresponding to a loss of more than 90% of their initial ductility. This pattern persisted at 48 h, where the difference among formulations remained highly significant (one-way ANOVA, $F = 156.31$, $p < 0.001$), with the blank retaining substantially higher elongation than any of the TiO_2-containing films.

As expected for conventional polyethylene, the control film exhibited a more gradual loss of ductility with increasing exposure time (Figure 9), consistent with the slower onset of oxidation already observed in its CI and Mass-Loss trends relative to the TiO_2-containing formulations. This apparent stability, however, did not persist at longer exposure times: by 72 h, the blank's elongation had collapsed abruptly, dropping to a similar level than that of TiO_2 1% (0.008 vs. 0.005 mm/mm, one-way ANOVA, $p < 0.001$), marking the point at which the previously more ductile control film underwent its own sharp embrittlement transition. At this same exposure time, TiO_2 2%, TiO_2-Pip 1%, and TiO_2-Pip 2% specimens had become too brittle to be mounted for tensile testing, precluding their inclusion in the statistical comparison; this loss of testable specimens is itself indicative of their more advanced degradation relative to the other two formulations.

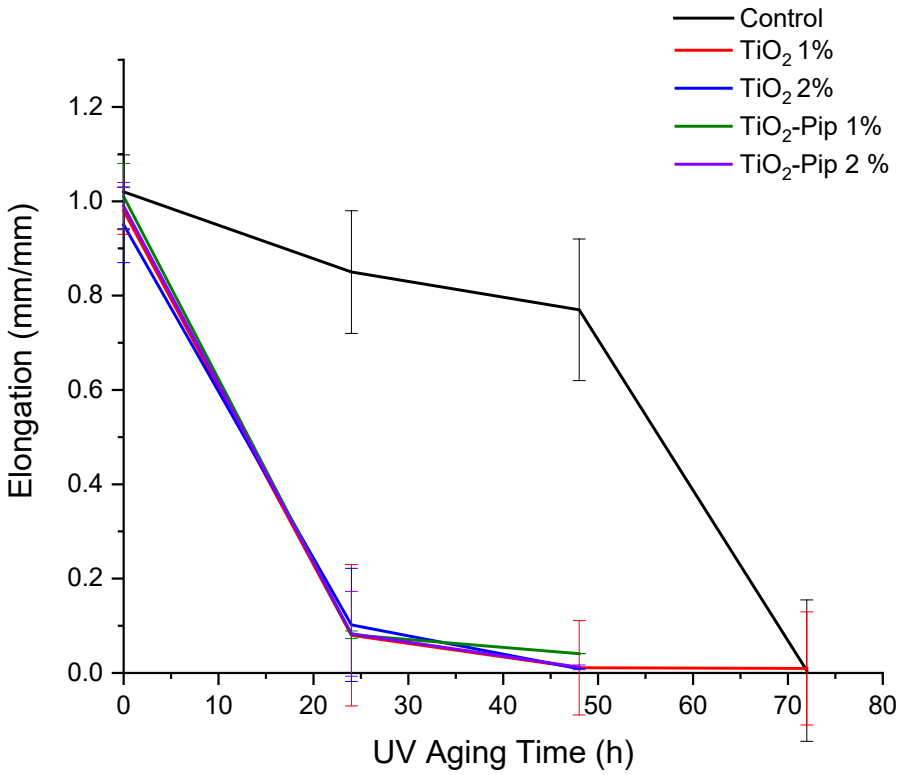


Figure 9. Loss of tensile properties of the polyethylene films formulated with the synthesized prodegradant additive at different aging periods of time.

The fact that the elongation curves for films containing pristine TiO_2 and TiO_2-Pip display similar trends throughout most of the aging period reinforces the idea that, regardless of mechanistic details, both systems converge toward the formation of highly oxidized and fragmented polymer structures with reduced capacity to withstand tensile

stress. For pristine TiO_2, the loss of elongation is primarily associated with the generation of hydroxyl radicals under UV irradiation, arising from electronic excitation processes on the oxide surface. In contrast, LDPE films containing TiO_2-Pip undergo an even more efficient degradation process, although the mechanical manifestation is similar: a rapid decline in elongation. The combination of inorganic photocatalysis and hydrogen abstraction is consistent with a more efficient degradation pathway that leads to a fast reduction in molecular weight and, consequently, a pronounced loss of elongation, although the relative contribution of each mechanism was not quantitatively deconvoluted in this study.

These findings are consistent with previous work from our research group, in which UV-aged LDPE films exhibited a rapid and pronounced loss of tensile properties within the first 24 h of exposure [20]. In that earlier study, the mechanical response deteriorated sharply during the initial stages of photo-oxidation, confirming that chain scission and embrittlement processes are initiated very early during UV irradiation. The present results reinforce this behavior, demonstrating that the onset of mechanical degradation occurs predominantly during the first day of UV aging.

3.5. SEM Micrographs of Degraded LDPE Films

Figure 10 presents the SEM micrographs of the LDPE films after 240 h of UV exposure. The control film (Figure 10a), which contains no additives, shows a relatively smooth surface with only minor irregularities. Although complementary analytical data indicate partial degradation, the micrograph reveals no major cracks or through-thickness damage. In contrast, the films containing pristine TiO_2 at 1 wt% and 2 wt% (Figure 10b,c) exhibit more evident signs of deterioration. Both micrographs show the formation of surface cracks and localized fracture lines, indicating increased embrittlement compared with the control. However, the damage remains mostly superficial, without extensive fragmentation. A more severe degradation pattern is observed in the films formulated with TiO_2-Pip at 1 wt% (Figure 10d). Here, the crack network is denser and deeper, suggesting that the piperonyl-modified TiO_2 accelerates the oxidative and mechanical deterioration of the polymer more effectively than pristine TiO_2 at higher loadings. The film containing TiO_2-Pip at 2 wt% (Figure 10e) shows the most pronounced damage. The micrograph reveals extensive fragmentation, and the fracture surfaces appear more granular, with clear through-thickness cracks, indicating severe embrittlement and structural failure. This morphology confirms that the highest concentration of the modified TiO_2 produces the strongest pro-degradant effect, leading to substantial physical and chemical deterioration of the LDPE matrix. Overall, the SEM analysis demonstrates a clear trend: TiO_2-Pip, particularly at 2 wt%, induces significantly greater degradation than pristine TiO_2, validating its role as an effective pro-oxidant additive under UV aging conditions.

Notably, the extent of surface damage follows the same order as the mass-loss discussed in Section 3.3.2: blank < 1 wt% pristine TiO_2 < 2 wt% pristine TiO_2 < 1 wt% TiO_2-Pip < 2 wt% TiO_2-Pip. The deep cracks, delamination and extensive fragmentation observed in the films containing TiO_2-Pip are consistent with the detachment of embrittled polymer fragments from the film surface. Similar crack formation, fragmentation and mass loss have been reported for photo-oxidized LDPE [45,46], where chain scission generates low-molecular-weight species that can either volatilize or detach from the surface as fragments. These observations support the interpretation that fragment detachment contributes to the higher mass loss of the films containing TiO_2-Pip.

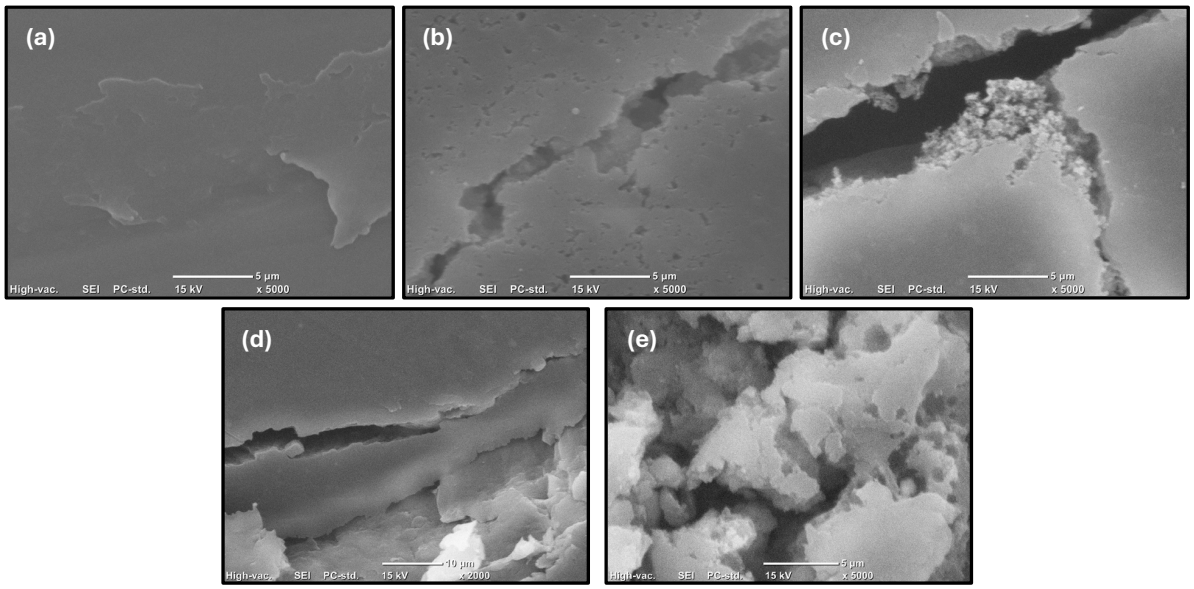


Figure 10. SEM micrographs of LDPE films after 240 h of UV aging: (**a**) blank LDPE film (no additives); (**b**) LDPE + 1 wt% pristine TiO_2; (**c**) LDPE + 2 wt% pristine TiO_2; (**d**) LDPE + 1 wt% TiO_2-Pip; (**e**) LDPE + 2 wt% TiO_2-Pip.

3.6. Determination of the Aerobic Biodegradability of Degraded LDPE Films Using Microorganisms

To assess whether the oxidized oligomers produced during the oxo-degradation of LDPE films formulated with TiO_2-Pip could support fungal colonization by microorganisms an aerobic biodegradability test was carried out following the ASTM D5247 standard. This protocol provides a controlled framework for determining whether microorganisms can use low-molecular-weight oxidation products as a carbon source, thereby establishing whether the degradation treatments applied to the films generate species that are metabolizable under aerobic conditions.

As expected, the positive control (MSM supplemented with glucose) supported vigorous growth of both *Aspergillus niger* ATCC 6275 and *Penicillium* sp. ATCC 52180. Extensive mycelial development was observed, forming aggregates of various sizes along with well-defined sporulating structures, confirming that the culture conditions were fully suitable for both fungal strains. In contrast, MSM lacking a carbon source and inoculated with the fungal strain (Negative Control 1) showed no growth, consistent with the fact that MSM contains mineral salts and nitrogen but requires an external carbon source to sustain fungal metabolism. Likewise, Negative Control 2 (MSM + degraded LDPE, non-inoculated) and Negative Control 3 (MSM + non-degraded LDPE, non-inoculated) exhibited no microbial development. Visual inspection and stereomicroscopy confirmed the absence of contamination, demonstrating that neither degraded nor pristine LDPE films supported spontaneous microbial proliferation during the exposure period.

A markedly different response was observed for the LDPE film containing 2% TiO_2-Pip and subjected to 240 h of UV aging, which exhibited a molecular weight of 3300 g/mol. After 30 days of exposure to *Aspergillus niger* and *Penicillium* sp., dense mycelial aggregates were clearly visible on the aged film (Figure 11). Microscopic examination confirmed extensive hyphal growth attached to the polymer surface. This behavior indicates that UV aging significantly reduces the molecular weight of LDPE, generating oxidized fragments that microorganisms can more readily assimilate. The images show compact mycelial clusters forming on the aged LDPE fragments, evidencing sustained fungal colonization throughout the exposure period. Higher-magnification micrographs (Figure 11c,f) reveal a dense network of branched hyphae adhering to the polymer surface, a characteristic

indicator of active fungal growth. The localized brownish pigmentation observed in these regions is consistent with fungal biomass accumulation. Similar biodegradation responses of LDPE exposed to *Aspergillus* species have been reported in the literature [50–52].

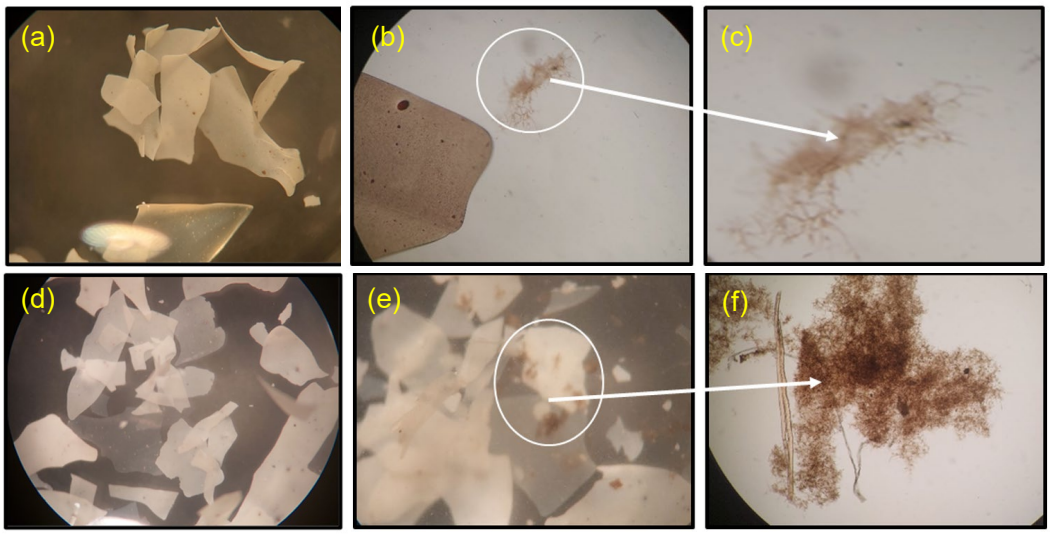


Figure 11. Microscopic evidence of fungal colonization on UV-aged LDPE films containing TiO_2-Pip. Micrographs of LDPE fragments subjected to a 30-day fungal culture: (**a**–**c**) samples exposed to *Penicillium* sp., showing regions colonized by dense mycelial aggregates; (**d**–**f**) samples exposed to *Aspergillus niger*.

Overall, these findings demonstrate that UV-aged LDPE containing TiO_2-Pip becomes significantly more susceptible to biodegradation under the evaluated conditions. In contrast, the non-aged LDPE film with 2% functionalized TiO_2 showed no detectable fungal growth after 30 days, as confirmed by visual inspection and stereomicroscopy, indicating that the untreated material remains resistant to microbial assimilation. It should be noted that the fungal assay performed in this study is based on qualitative microscopic monitoring of mycelial growth on the film surface, and does not by itself constitute direct, quantitative proof of carbon assimilation or mineralization. Confirmation of true bioassimilation would require complementary quantitative assays, such as CO_2 evolution (mineralization percentage, e.g., ISO 14852:2021 [53]), Total Organic Carbon (TOC) reduction, or fungal biomass dry-weight tracking, which are beyond the scope of the present study and are proposed as a direction for future work.

3.7. Comparison of This Work with Previously Reported TiO_2-Based Pro-Degradant Systems

To place these results in context, Table 2 compares the degradation performance of TiO_2-Pip with our previously reported fatty-acid-modified TiO_2 additives [20] and with other organically modified TiO_2 pro-degradant systems reported in the literature. To our knowledge, the five entries in Table 2, namely, our previously reported fatty-acid-modified TiO_2 additives [20] and the three literature reports by Yang et al. [33], Xu et al. [34], and Zapata-Tello et al. [35], represent the complete set of studies identified in a systematic literature search that specifically employ an organically functionalized TiO_2 as a pro-degradant additive for polyethylene and report a quantitative measure of degradation (GPC-derived Mw/Mn and/or CI) together with some form of biological assay. No other reports combining these three elements, namely, organic functionalization of TiO_2, a polyethylene matrix, and a quantitative and/or biological degradation assessment, were identified. We therefore consider this table to reflect the full set of directly comparable studies available in literature, rather than a selective illustration.

Table 2. Degradation performance of TiO_2-Pip compared with previously reported organically modified TiO_2 pro-degradant systems for LDPE.

#	System	Organic Modifier	Polymer	UV Conditions	Reported Results
1	This work	Piperonyl maleate	LDPE	240 h	Mw: 88,782 → 3353 g/mol (2%, 96.2%); Observed fungal colonization after 30 days
2	Previous work ref. [20]	Arachidonic and Cervonic acid	LDPE	200	Mw: 95,000 → 4880 g/mol (3%, ≈−94.9%) No bioassimilation studies were performed.
3	Xu et al., ref. [33]	PEG-modified TiO_2	LDPE	370 h	Decrease in Mw to 30,402 g/mol. Observed fungal colonization after 180 days. Mineralization of only 16% occurred in this time.
4	Yang et al., ref. [34]	Grafted-PMMA TiO_2 (12, 25 and 45%)	LDPE	415 h	Decrease in Mw of 46.3%, 87.5% and 97%. Qualitative data reported on fungal colonization observed in films with TiO_2/PMMA after UV aging.
5	Zapata-Tello et al., ref. [35]	Dicarboxylic-acid-modified TiO_2	LDPE	336 h	GPC data is not reported. Pristine TiO_2 displayed the highest CI, followed by glutaric acid–TiO_2. No bioassmilation studies were performed.

Within this set, TiO_2-Pip achieves one of the largest reductions in molecular weight reported (96.2%, decreased Mw from 88,782 to 3353 g/mol) at only 2 wt% loading, within 240 h of UV exposure. Our previously reported fatty-acid-modified TiO_2 additives [20] reach a very similar magnitude of reduction (94.9%, at 200 h) but require a higher loading (3 wt%) and, critically, were not accompanied by any biological assays, a gap that the present work directly addresses. Yang et al. [33] require both a much longer UV exposure (415 h, i.e., 73% longer than in this study) and a very high organic grafting density (45%) to reach a comparable reduction (97%); at more moderate grafting levels (12% and 25%), their system reaches only 46.3% and 87.5% reduction in Mw, respectively, well below TiO_2-Pip's performance at less than half the exposure time. Xu et al.'s [34] PEG-modified TiO_2 shows a markedly shallower abiotic stage (final Mw of 30,402 g/mol after 370 h) and a much slower biological response, with fungal colonization appearing only after 180 days (six times longer than the 30 days observed for TiO_2-Pip) and reaching just 16% mineralization in that time. Zapata-Tello et al. [35] did not reach the point of reporting GPC data at all, relying on the Carbonyl Index alone, and notably found that unmodified TiO_2 outperformed their dicarboxylic-acid-modified TiO_2 in CI, illustrating that organic modification of TiO_2 does not automatically translate into improved pro-degradant activity, and no bioassimilation studies were performed in that system either.

Taken together, across the full set of directly comparable systems identified in the literature, TiO_2-Pip is the only one that combines (i) a substantial reduction in molecular weight, (ii) the shortest UV exposure time required to reach it, and (iii) direct evidence of fungal colonization on a markedly shorter timescale than any other reported system. This combined abiotic–biotic performance supports the conclusion that the piperonyl-maleate modification offers a genuine, quantifiable improvement over both our own previously reported fatty-acid-based TiO_2 additives and over all other organically modified TiO_2 pro-degradant systems for polyethylene reported to date.

A methodological limitation should be acknowledged regarding the film geometry used in this study (150 µm blown LDPE, QUV-aged), which differs from environmental microplastic particles in surface-area-to-volume ratio and photon penetration depth, factors

expected to influence degradation rate and depth. These results should therefore be interpreted as demonstrating the pro-degradant chemistry of TiO_2-Pip under controlled, film-based conditions. Testing micronized LDPE powder is identified as the appropriate next step to evaluate whether these efficiency gains extend to microplastic substrates.

4. Conclusions

This work demonstrates an effective strategy for accelerating the oxo-degradation of polyolefins by engineering TiO_2 surfaces with organic moieties bearing highly labile hydrogens. Functionalization of TiO_2 with the monoester PipM, supported by FTIR, XPS, TGA, and EDS characterization, produced a hybrid photocatalyst, TiO_2-Pip, that markedly accelerated LDPE chain scission relative to pristine TiO_2, reducing Mw from 88,000 to 3353 g/mol after 240 h of UV exposure, within the range reported as microbially assimilable. We propose that this enhanced activity arises from abstraction of the labile benzylic and acetalic hydrogens on the piperonyl moiety, with the maleate double bond potentially contributing to radical chain propagation; this mechanism is supported by established structure–reactivity precedents but has not been directly confirmed (e.g., by EPR) and should be regarded as a working hypothesis for future verification. Biodegradation assays showed that only the UV-aged TiO_2-Pip films supported visible fungal colonization by *Aspergillus niger* and *Penicillium* sp., indicating that abiotic oxidation is a precondition for microbial interaction; as this qualitative assay does not confirm assimilation or mineralization, quantitative validation (e.g., CO_2 evolution and TOC reduction) is proposed for future work. It should also be noted that degradation in this study was assessed under accelerated QUV aging with an irradiance considerably more intense than natural sunlight; the degradation rates reported here are therefore not expected to translate directly to real-world weathering timescales, and validation under natural outdoor exposure is needed to establish realistic degradation rates. Together, these results position TiO_2-Pip as a promising laboratory-scale platform for accelerating the oxidative fragmentation of LDPE.

Author Contributions: Conceptualization, R.A.O.; Methodology, R.A.O., R.Y.M., H.M.T., V.J.C.D., A.S.L.P. and A.E.G.V.; Validation, R.A.O., R.Y.M., H.M.T., V.J.C.D., A.S.L.P. and A.E.G.V.; Formal Analysis, R.A.O.; Investigation, R.Y.M., H.M.T., V.J.C.D., A.S.L.P. and A.E.G.V.; Resources, R.A.O.; Data Curation, R.A.O.; Writing—Original, Draft Preparation, R.A.O.; Writing—Review and Editing, R.A.O.; Visualization, R.A.O. and R.Y.M.; Supervision, R.A.O.; Project Administration, R.A.O.; Funding Acquisition, R.A.O. All authors have read and agreed to the published version of the manuscript.

Funding: This research was funded by CIQA, grant number 6777.

Institutional Review Board Statement: Not applicable.

Data Availability Statement: Data is contained within the article.

Acknowledgments: The authors extend their appreciation to Maria Guadalupe Mendez, Israel Sifuentes, Gilberto Hurtado, Jesus Cepeda, Alfonso Mercado, and Jesús Francisco Lara, for their valuable collaboration in sample analysis, characterization and the mechanical testing of the films.

Conflicts of Interest: The authors declare no conflicts of interest.

References

1. Lu, P.-Y.; Ningsih, L.A.; Heksa, A.C.; Hu, C.-C.; Chen, W.-C.; Chiu, Y.-C. Solid base-assisted photocatalytic degradation of polyethylene via the Norrish mechanism through the generation of alternating polyketones. *Polym. J.* **2025**, *57*, 575–586. [CrossRef]
2. Nabi, I.; Bacha, A.-U.-R.; Ahmad, F.; Zhang, L. Application of titanium dioxide for the photocatalytic degradation of macro-and micro-plastics: A review. *J. Environ. Chem. Eng.* **2021**, *9*, 105964. [CrossRef]
3. Zhang, J.; Nosaka, Y. Mechanism of the OH radical generation in photocatalyst with TiO_2 of different crystalline types. *J. Phys. Chem. C* **2014**, *118*, 10824–10832. [CrossRef]

4. Nosaka, Y.; Nosaka, A. Understanding hydroxy radicals (.OH) generation process in photocatalyst. *ACS Energy Lett.* **2016**, *1*, 356–359. [CrossRef]
5. Islam, N.M.; Othman, N.; Ahmad, Z.; Ismail, H. Effect of prodegradant additives concentration on aging properties of polypropylene films. *Polym.-Plast. Technol.* **2010**, *49*, 272–278. [CrossRef]
6. Zapata, P.A.; Zenteno, A.; Amigó, N.; Rabagliati, F.M.; Sepúlveda, F.; Catalina, F.; Corrales, T. Study on the photodegradation of nanocomposites based on polypropylene and TiO_2 nanotubes. *Polym. Degrad. Stab.* **2016**, *133*, 101–107. [CrossRef]
7. Davidson, R.S.; Meek, R.R. The photodegradation of polyethylene and polypropylene in the presence and absence of added titanium dioxide. *Eur. Polym. J.* **1981**, *17*, 163–167. [CrossRef]
8. Zan, L.; Fa, W.; Wang, S. Novel Photodegradable Low-Density Polyethylene-TiO_2 Nanocomposite Film. *Environ. Sci. Technol.* **2006**, *40*, 1681–1685. [CrossRef]
9. Vazquez, Y.V.; Ressia, J.A.; Cerrada, M.L.; Barbosa, S.E.; Vallés, E.M. Prodegradant Additives Effect onto Commercial Polyolefins. *J. Polym. Environ.* **2019**, *27*, 464–471. [CrossRef]
10. Ohtani, B.; Adzuma, S.; Nishimoto, S.; Kagiya, T. Photocatalytic degradation of polyethylene film by incorporated extra-fine particles of titanium dioxide. *Polym. Degrad. Stab.* **1992**, *35*, 53–60. [CrossRef]
11. Verma, R.; Singh, S.; Dalai, M.K.; Saravanan, M.; Agrawal, V.V.; Srivastava, A.K. Photocatalytic degradation of polypropylene film using TiO_2-based nanomaterials under solar irradiation. *Mater. Des.* **2017**, *133*, 10–18. [CrossRef]
12. Zaman, A.; Kausar, A.; Asim, S.; Mansha, A. Modified TiO_2 and ZnO photocatalysts for microplastic degradation: Mechanisms, challenges, and recent advances. *Photochem. Photobiol. Sci.* **2026**, *25*, 765–789. [CrossRef]
13. He, Y.; Rehman, A.U.; Xu, M.; Not, C.A.; Ng, A.M.C.; Djurisic, A.B. Photocatalytic degradation of different types of microplastics by TiOx/ZnO tetrapod photocatalysts. *Heliyon* **2023**, *9*, e22562. [CrossRef]
14. Silva, D.B.; Marques, A.C. TiO_2-based photocatalytic degradation of microplastics in water: Current status, challenges and future perspectives. *J. Water Process Eng.* **2025**, *72*, 107465. [CrossRef]
15. Llorente-Garcia, B.E.; Hernandez-Lopez, J.M.; Zaldivar-Cadena, A.A.; Siligardi, C.; Cedillo-Gonzalez, E.I. First Insights into Photocatalytic Degradation of HDPE and LDPE Microplastics by a Mesoporous N–TiO_2 Coating: Effect of Size and Shape of Microplastics. *Coatings* **2020**, *10*, 658. [CrossRef]
16. Nabi, I.; Bacha, A.-U.-R.; Li, K.; Cheng, H.; Wang, T.; Liu, Y.; Ajmal, S.; Yang, Y.; Feng, Y.; Zhang, L. Complete Photocatalytic mineralization of microplastics in TiO_2 nanoparticles film. *iScience* **2020**, *23*, 101326. [CrossRef]
17. Yeszhan, Y.; Bexeitova, K.; Yermekbayev, S.; Toktarbay, Z.; Lee, J.; Berndtsson, R.; Azat, S. Photocatalytic Degradation of Microplastics in Aquatic Environments: Materials, Mechanisms, Practical Challenges, and Future Perspectives. *Water* **2025**, *17*, 2139. [CrossRef]
18. Jung, Y.J.; Kim, I.Y. Recent advances and protocol summaries for degradation of polyethylene microplastics using TiO_2-based photocatalysts. *Bull. Korean Chem. Soc.* **2025**, *46*, 198. [CrossRef]
19. Turner, A.; Filella, M. The role of titanium dioxide on the behaviour and fate of plastics in the aquatic environment. *Sci. Total Environ.* **2023**, *869*, 161727. [CrossRef]
20. Acosta Ortiz, R.; Yañez Macías, R.; Gómez Alfaro, K.; Cruz Delgado, V.J.; Rodríguez Gonzalez, F.; Ku Herrera, J.J.; Garcia Valdez, A.E. Synthesis of two TiO_2-based prodegradant additives and their efficiency in inducing the accelerated photo-oxidation of low-density polyethylene. *Polym. Degrad. Stab.* **2024**, *224*, 110753. [CrossRef]
21. Albertsson, A.-C.; Karlsson, S. The influence of biotic and abiotic environments on the degradation of polyethylene. *Prog. Polym. Sci.* **1990**, *15*, 177–192. [CrossRef]
22. Hakkarainen, M.; Albertsson, A.C. Environmental Degradation of Polyethylene. In *Long Term Properties of Polyolefins*; Albertsson, A.C., Ed.; Advances in Polymer Science; Springer: Berlin/Heidelberg, Germany, 2004; Volume 169. [CrossRef]
23. Albertsson, A.-C.; Andersson, S.O.; Karlsson, S. The mechanism of biodegradation of polyethylene. *Polym. Degrad. Stab.* **1987**, *18*, 73–87. [CrossRef]
24. Ojeda, T.F.M.; Dalmolin, E.; Forte, M.M.C.; Jacques, R.J.S.; Bento, F.M.; Camargo, F.A.O. Abiotic and biotic degradation of oxo-biodegradable polyethylene. *Polym. Degrad. Stab.* **2009**, *94*, 965–970. [CrossRef]
25. Chiellini, E.; Corti, A.; D'Antone, S. Oxo-biodegradable full carbon backbone polymers- biodegradation behaviour of thermally oxidized polyethylene in an aqueous medium. *Polym. Degrad. Stab.* **2007**, *92*, 1378–1383. [CrossRef]
26. Lucas, N.; Bienaime, C.; Belloy, C.; Queneudec, M.; Silvestre, F.; Nava-Saucedo, J.-E. Polymer biodegradation: Mechanisms and estimation techniques. *Chemosphere* **2008**, *73*, 429–442. [CrossRef]
27. Roy, P.K.; Surekha, P.; Rajagopal, C.; Chatterjee, S.N.; Choudhary, V. Studies on the photo-oxidative degradation of LDPE films in the presence of oxidised polyethylene. *Polym. Degrad. Stab.* **2007**, *92*, 1151–1160. [CrossRef]
28. Gewert, B.; Plassmann, M.M.; MacLeod, M. Pathways for degradation of plastic polymers floating in the marine environment. *Environ. Sci. Process. Impacts* **2015**, *17*, 1513–1521. [CrossRef]
29. Shah, A.A.; Hasan, F.; Hameed, A.; Ahmed, S. Biological degradation of plastics: A comprehensive review. *Biotechnol. Adv.* **2008**, *26*, 246–265. [CrossRef]

30. Restrepo-Flórez, J.-M.; Bassi, A.; Thompson, M.R. Microbial degradation and deterioration of polyethylene, A review. *Int. Biodeterior. Biodegrad.* **2014**, *88*, 83–90. [CrossRef]
31. Ghatge, S.; Yang, Y.; Ahn, J.-H.; Hur, H.-G. Biodegradation of polyethylene: A brief review. *Appl. Biol. Chem.* **2020**, *63*, 27. [CrossRef]
32. Narancic, T.; O'Connor, K.E. Plastic waste as a global challenge: Are biodegradable plastics the answer? *Microbiology* **2019**, *165*, 129–137. [CrossRef]
33. Xu, J.; Yang, W.; Zhang, C.; Dong, X.; Luo, Y. Photo-Oxidation and Biodegradation of Polyethylene Films Containing Polyethylene Glycol Modified TiO_2 as Pro-Oxidant Additives. *Polym. Compos.* **2018**, *39*, E531–E539. [CrossRef]
34. Yang, W.; Song, S.; Zhang, C.; Liang, W.; Dong, X.; Luo, Y.; Cai, X. Enhanced Photocatalytic Oxidation and Biodegradation of Polyethylene Films with PMMA Grafted TiO_2 as Pro-Oxidant Additives for Plastic Mulch Application. *Polym. Compos.* **2018**, *39*, 3409–3417. [CrossRef]
35. Zapata-Tello, D.L.; Escobar-Barrios, V.; Gonzalez-Calderon, J.A.; Perez, E. Chemical modification of titanium dioxide nanoparticles with dicarboxylic acids to mediate the UV degradation in polyethylene films. *Polym. Bull.* **2020**, *77*, 6409–6431. [CrossRef]
36. *ASTM G154-23*; Standard Practice for Operating Fluorescent Ultraviolet (UV) Lamp Apparatus for Exposure of Materials. ASTM International: West Conshohocken, PA, USA, 2023.
37. *ASTM D882-18*; Standard Test Method for Tensile Properties of Thin Plastic Sheeting. ASTM International: West Conshohocken, PA, USA, 2018.
38. *ASTM D5247-92*; Standard Test Method for Determining the Aerobic Biodegradability of Degradable Plastics by Specific Microorganisms. ASTM International: West Conshohocken, PA, USA, 1992.
39. Abdullah, S.; Maroof, L.; Iqbal, M.; Farman, S.; Lubna, S.F. Biodegradation of Low-Density Polyethylene (LDPE) Bags by Fungi Isolated from Waste Disposal Soil. *Appl. Environ. Soil Sci.* **2022**, 8286344. [CrossRef]
40. Wang, X.; Zhang, L. Kinetic study of hydroxy radicals formation in a continuous hydroxyl generation system. *RSC Adv.* **2018**, *8*, 40632–40638. [CrossRef]
41. Blanksby, S.J.; Ellison, G.B. Bond Dissociation Energies of Organic Molecules. *Acc. Chem. Res.* **2003**, *36*, 255–263. [CrossRef]
42. Le Calvé, S.; Mellouki, A.; Le Bras, G. Kinetic studies of OH reactions with propylal, butylal and 1,3-dioxolane. *Phys. Chem. Chem. Phys.* **2002**, *4*, 5622–5626. [CrossRef]
43. Moad, G. The synthesis of polyolefin graft copolymers by reactive extrusion. *Prog. Polym. Sci.* **1999**, *24*, 81–142. [CrossRef]
44. Xiao, C.; Li, S.; Yi, F.; Zhang, B.; Chen, D.; Zhang, Y.; Chen, H.; Huang, Y. Enhancement of photo-Fenton catalytic activity with the assistance of oxalic acid on the kaolin–FeOOH system for the degradation of organic dyes. *RSC Adv.* **2020**, *10*, 18704–18714. [CrossRef]
45. El Kharraf, A.; Rabiller-Baudry, M.; Pradas Del Real, A.; Sandt, C.; Wiesner, M.; Nemeth, G.; Bavay, D.; Peraza Ku, S.; Bossa, N.; Davranche, M. Polyethylene plastic degradation: The dual pathways from macroplastics to nanoplastics. *J. Hazard. Mater.* **2025**, *499*, 140200. [CrossRef]
46. Arredondo-Navarro, A.; Gallardo-Owens, D.; Scott, J.; Farias, S.; Wang, X.; Cochran, W.; El Hayek, E.; Minghetti, M.; Cerrato, J.M.; Gonzalez-Estrella, J. Thermal oxidation, ultraviolet radiation, and mechanical abrasion—Understanding mechanisms of microplastic generation and chemical transformation. *Microplast. Nanoplast.* **2026**, *6*, 26. [CrossRef]
47. White, J.R.; Shyichuk, A.V. Macromolecular scission and crosslinking rate changes during polyolefin photo-oxidation. *Polym. Degrad. Stab.* **2007**, *92*, 1161–1168. [CrossRef]
48. Craig, I.H.; White, J.R.; Shyichuk, A.V.; Syrotynska, I. Photo-induced scission and crosslinking in LDPE, LLDPE, and HDPE. *Polym. Eng. Sci.* **2005**, *45*, 579–587. [CrossRef]
49. Amin, M.U.; Scott, G.; Tillekeratne, L.M.K. Mechanism of the photo-initiation process in polyethylene. *Eur. Polym. J.* **1975**, *11*, 85–89. [CrossRef]
50. DSouza, G.C.; Sheriff, R.S.; Ullanat, V.; Shrikrishna, A.; Joshi, A.V.; Hiremath, L.; Entoori, K. Fungal Biodegradation of low-density polyethylene using consortium of Aspergillum Niger under controlled conditions. *Heliyon* **2021**, *7*, e07008. [CrossRef]
51. Munir, E.; Harefa, R.S.M.; Priyani, N.; Suryanto, D. Plastic degrading fungi Trichoderma viride and Aspergillus nomius isolated from local landfill soil in Medan. *IOP Conf. Ser. Earth Environ. Sci.* **2018**, *126*, 012145. [CrossRef]
52. Ogunbayo, A.O.; Olanipekun, O.O.; Adamu, I.A. Preliminary Studies on the Microbial Degradation of Plastic Waste Using *Aspergillus niger* and *Pseudomonas* sp. *J. Environ. Prot.* **2019**, *10*, 625–631. [CrossRef]
53. *ISO 14852:2021*; Determination of the Ultimate Aerobic Biodegradability of Plastic Materials in an Aqueous Medium—Method by Analysis of Evolved Carbon Dioxide. International Organization for Standardization (ISO): Geneva, Switzerland, 2021.

Disclaimer/Publisher's Note: The statements, opinions and data contained in all publications are solely those of the individual author(s) and contributor(s) and not of MDPI and/or the editor(s). MDPI and/or the editor(s) disclaim responsibility for any injury to people or property resulting from any ideas, methods, instructions or products referred to in the content.